

**Universidade Federal do Rio Grande - FURG**

**Instituto de Oceanografia**

Programa de Pós-Graduação em Oceanologia

# **Variação sazonal da capacidade tampão do pH no sul do estuário da lagoa dos Patos**

**Paco Luisyn Quintana Effio**

Dissertação apresentada ao Programa  
de Pós-Graduação em Oceanologia,  
como parte dos requisitos para a  
obtenção do Título de Mestre.

Orientador: *Profa. Dra. Eunice da Costa Machado*

Universidade Federal do Rio Grande (FURG), Brasil.

Co-orientador: *Prof. Dr. Rodrigo Kerr Duarte Pereira*

Universidade Federal do Rio Grande (FURG), Brasil.

Rio Grande, RS, Brasil

Julho 2023

# **Variação sazonal da capacidade tampão do pH no sul do estuário da lagoa dos Patos**

Dissertação apresentada ao Programa de Pós-Graduação em Oceanologia,  
como parte dos requisitos para a obtenção do Título de Mestre.

Por

**Paco Luisyn Quintana Effio**

Rio Grande, RS, Brasil

Julho 2023

© A cópia parcial e a citação de trechos desta tese são permitidas sobre a condição de que qualquer pessoa que a consulte reconheça os direitos autorais do autor. Nenhuma informação derivada direta ou indiretamente desta obra deve ser publicada sem o consentimento prévio e por escrito do autor.

## Ficha Catalográfica

Q7v Quintana Effio, Paco Luisyn.  
Variação sazonal da capacidade tampão do pH no sul do estuário da Lagoa dos Patos / Paco Luisyn Quintana Effio. – 2023.  
70 f.

Dissertação (mestrado) – Universidade Federal do Rio Grande – FURG, Programa de Pós-Graduação em Oceanologia, Rio Grande/RS, 2023.  
Orientadora: Dra. Eunice da Costa Machado.  
Coorientador: Dr. Rodrigo Kerr Duarte Pereira.

1. Capacidade tampão 2. Acidificação estuarina 3. Ambiente costeiro 4. Lagoa dos Patos I. Machado, Eunice da Costa II. Pereira, Rodrigo Kerr Duarte III. Título.

CDU 551.46

Catálogo na Fonte: Bibliotecário José Paulo dos Santos CRB 10/2344



## ATA ESPECIAL DE DEFESA DE DISSERTAÇÃO DE MESTRADO – 02/2023

Às nove horas do dia 06 de julho do ano dois mil e vinte e três, por Vídeo Conferência, reuniu-se a Comissão Examinadora da Dissertação de **MESTRADO** intitulada " **VARIAÇÃO SAZONAL DA CAPACIDADE TAMPÃO DO PH NO SUL DO ESTUÁRIO DA LAGOA DOS PATOS**", do **Acad. Paco Luisyn Quintana Effio**. A Comissão Examinadora foi composta pelos seguintes membros: Profa. Dra. Eunice Machado – Orientadora – (IO/FURG), Prof. Dr. Rodrigo Kerr - (Coorientador - IO/FURG), Prof. Dr. Carlos Francisco Ferreira de Andrade – (IO/FURG), Profa. Dra. Alessandra Larissa de Oliveira Fonseca – (UFSC) e Prof. Dr. Ozelito Possidônio de Andrade Jr. – (IFMA). Dando início à reunião, a coordenadora do PPGO, Profa. Dra. Grasiela Lopes Leães Pinho, agradeceu a presença de todos e fez a apresentação da Comissão Examinadora. Logo após esclareceu que o Candidato teria um tempo de 45 a 60 min para explanação do tema, e cada membro da Comissão Examinadora, um tempo máximo de 30 min para perguntas. A seguir, passou à palavra ao Candidato que apresentou o tema e respondeu às perguntas formuladas. Após ampla explanação, a Comissão Examinadora reuniu-se em reservado para discussão do conceito a ser atribuído ao Candidato. Foi estabelecido que as sugestões de todos os membros da Comissão Examinadora, que seguem em pareceres em anexo, foram aceitas pelo Orientador/Candidato para incorporação na versão final da Dissertação. Finalmente, a Comissão Examinadora considerou o candidato **aprovado**, por unanimidade. Nada mais havendo a tratar, foi lavrada a presente ATA que após lida e aprovada, será assinada pela Comissão Examinadora, pelo Candidato e pela Coordenadora do Programa de Pós-Graduação em Oceanologia.

Documento assinado digitalmente



EUNICE DA COSTA MACHADO  
Data: 04/07/2023 09:01:41-0300  
Verifique em <https://validar.iti.gov.br>

Profa. Dra. Eunice da Costa Machado  
Orientador

Documento assinado digitalmente



RODRIGO KERR DUARTE PEREIRA  
Data: 17/07/2023 11:17:43-0300  
Verifique em <https://validar.iti.gov.br>

Prof. Dr. Rodrigo Kerr  
Coorientador

Documento assinado digitalmente



CARLOS FRANCISCO FERREIRA DE ANDRAI  
Data: 12/07/2023 14:28:51-0300  
Verifique em <https://validar.iti.gov.br>

Prof. Dr. Carlos Francisco Ferreira de Andrade



Documento assinado digitalmente

Alessandra Larissa D Oliveira Fonseca  
Data: 06/07/2023 13:03:17-0300  
CPF: \*\*\*.350.779-\*\*  
Verifique as assinaturas em <https://v.ufsc.br>

Profa. Dra. Alessandra Larissa de O. Fonseca

Documento assinado digitalmente



OZELITO POSSIDONIO DE AMARANTE JUN  
Data: 11/07/2023 14:38:50-0300  
Verifique em <https://validar.iti.gov.br>

Prof. Dr. Ozelito Possidônio de Amarante Jr.



Documento assinado digitalmente  
GRASIELA LOPES LEAES PINHO  
Data: 28/06/2023 15:33:18-0300  
Verifique em <https://validar.iti.gov.br>

Profª. Drª. Grasiela Lopes Leães Pinho  
Coordenadora PPGO

Acad. Paco Luisyn Quintana Effio

*In memoriam of Dr. Wilmer Carbajal Villalta*

# Agradecimientos

Resiliência é a palavra que descreve a humanidade nos últimos anos. Nossa capacidade de resistir, adaptar e superar qualquer adversidade apoiando-nos como seres sociais que somos por natureza. Resiliência foi a palavra que iniciou este caminho de crescimento.

A Juan y Pilar, mis padres, cuyo sacrificio, dedicación y unión superan cualquier adversidad. Mis padres, modelo de vida y pilar de nuestra formación y educación. Mis padres, quienes sin titubear acompañan nuestros pasos cada día siendo nuestro soporte para recorrer nuestro propio sendero y cuyo ejemplo nos demuestran que debemos seguir avanzando con fe y dedicación.

Rosa e Juana, mis abuelas, mi paz y mi tranquilidad, mi rincón de hogar que fortalecieron mi corazón y mente. Mi Mamá Juana y Mamá Rosa, cuyos recuerdos se convierten en breves historias que me sacan sonrisas pese al pasar del tiempo.

A mis hermanos, Juan y Cristhian, con su apoyo incondicional e inesperado durante uno de los momentos más vulnerables de mi vida. Prometo responder con la fortaleza y este es el primer paso para una revolución en mi vida.

A Mayte, Raquel, Mary, Cori, Raif, José y Alejandro, mi familia inesperada en un país acogedor. Nuestra añoranza y “saudade” por nuestras tierras nos permitieron conectar rápidamente y llamarnos hermanos y estar presente en las buenas, malas y peores.

A Edwin y Chris, mis amigos, compatriotas y hermanos. Su apoyo desde el inicio fue esencial, guiándome y auxiliándome en todo este proceso académico. Gracias por compartir toda sus experiencias.

Aos meus amigos Elis, Luiza, Sophia, Anderson, Raul, Brendon, Brenno, Luis e Andrés por oferecer sempre seu apoio acadêmico e pessoal, pela ajuda nos momentos difíceis, por me acolher e me integrar neste excelente grupo e família de pesquisadores.

Aos meus orientadores por todo seu apoio e paciência. Por me orientar e me ajudar sem hesitar durante este caminho de crescimento acadêmico e pessoal. Sua dedicação acadêmica é inspiração e modelo que espero, com esforço, replicar. Ao chegar nesse momento, numa pesquisa futura, espero dizer-lhes com um sorriso de gratidão, bom dia queridos professores e colegas!

Agradeço a todas as instituições que permitiram que este projeto fosse possível: CAPES, Universidade Federal de Rio Grande (FURG) e ao Programa de Pós-graduação em Oceanologia.

A todos aquellos que de alguna u otra forma colaboraron con esta experiencia. Mil gracias Brasil.

# Índice

<b>Agradecimentos</b> .....	<b>i</b>
<b>Lista de Figuras</b> .....	<b>v</b>
<b>Lista de Tabelas</b> .....	<b>ix</b>
<b>Lista de Acrônimos e Abreviações</b> .....	<b>x</b>
<b>Resumo</b> .....	<b>xii</b>
<b>Abstract</b> .....	<b>xiv</b>
<b>Capítulo I: Introdução</b> .....	<b>1</b>
<b>Capítulo II: Objetivos</b> .....	<b>10</b>
<b>Capítulo III: Área de estudo</b> .....	<b>11</b>
<b>Capítulo IV: Material e Métodos</b> .....	<b>14</b>
<b>Capítulo V: Resultados e Discussão</b> .....	<b>22</b>
<b>1. Introduction</b> .....	<b>23</b>
1.2. Patos Lagoon Estuary.....	27
<b>2. Material and Methods</b> .....	<b>29</b>
2.1. Sampling strategy.....	29
2.2. Temperature, salinity, nutrients and chlorophyll a.....	30
2.3. Total alkalinity and pH.....	31
2.4. Data processing and statistical analysis.....	32
2.5. Sensitivity factor and buffer capacity.....	34
2.6. Maximum Estuarine Acidification Salinity.....	35
2.7. Drivers of pH variability.....	36
<b>3. Results</b> .....	<b>37</b>
3.1. Statistical analysis.....	37
3.2. Sensitivity factor and buffer capacity.....	40

3.3. Maximum Estuarine Acidification Salinity.....	45
3.4. Drivers of pH.....	45
<b>4. Discussion.....</b>	<b>46</b>
<b>5. Concluding remarks.....</b>	<b>51</b>
<b>6. Declaration of competing interest.....</b>	<b>53</b>
<b>7. Data availability.....</b>	<b>54</b>
<b>8. Acknowledgments.....</b>	<b>54</b>
<b>9. Supplementary material.....</b>	<b>55</b>
<b>Capítulo VI: Síntese da Discussão e Conclusões.....</b>	<b>60</b>
<b>Referências bibliográficas.....</b>	<b>63</b>

# Lista de Figuras

## CAPÍTULO I:

- Figura 1.** Distribuição cumulativa de decréscimo nas tendências de pH em 83 sistemas costeiros, em comparação com decréscimos nas estações dos projetos de Estudo de Séries Temporais Atlântico das Bermudas (BATS) e Oceano de Hawaii (HOT) (acidificação do oceano - OA), e a gama de decréscimos oceânicos reportados na literatura (linhas tracejadas). Sistemas costeiros com baixo tamponamento são marcados com triângulos. As barras de erro mostram o intervalo de confiança de 95% das reduções de pH costeiras estimadas. Observe que as barras de erro OA são menores que os símbolos. Figura modificada de Carstensen & Duarte [2019].....**2**
- Figura 2.** Séries temporais de alcalinidade nos rios estadunidenses Mississippi (a), rio Delaware (b) e rios suecos (c). As linhas sólidas representam uma média móvel de 5 anos das concentrações médias anuais. Figura modificada de Duarte et al [2013].....**3**
- Figura 3.** Diagrama de dispersão da alcalinidade total (TA;  $\mu\text{mol kg}^{-1}$ ) e do carbono inorgânico total dissolvido (DIC;  $\mu\text{mol kg}^{-1}$ ). O diagrama TA-DIC-salinidade considera o conjunto de dados da rede BrOA, abrangendo o período entre maio de 2017 e junho de 2021, com verão representado por pontos, outono por triângulos, inverno por quadrados e primavera por losangos. As setas inseridas mostram os principais processos (conforme indicado), adaptados de Zeebe e Wolf-Gladrow (2007), que regem a variabilidade no sistema carbonato do estuário da lagoa dos Patos. A linha preta tracejada representa a linha de mistura conservativa teórica de águas fluviais e oceânicas que indicam o efeito da diluição e concentração de sal na mudança das concentrações de TA-DIC. As cruces roxa e vermelha representam os membros extremos das águas fluviais e oceânicas. A linha tracejada vermelha representa a curva de regressão linear do conjunto de dados. Figura modificada de Albuquerque et al. [2022].....**6**

### **CAPÍTULO III**

**Figura 1.** Mapa da zona estuarina inferior do Estuário da Lagoa dos Patos (esquerda) com localização das estações de monitoramento fixas no cais BrOA-1 e BrOA-2 (pontos amarelos). Os mapas da direita mostram a localização da zona estuarina da Lagoa dos Patos (parte superior) e do Estado do Rio Grande do Sul (parte inferior), ambas marcadas como retângulos vermelhos.....**13**

### **CAPÍTULO V**

**Figure 1.** Map of the lower estuarine zone of the Patos Lagoon Estuary (left) with the location of pier-fixed monitoring stations BrOA-1 and BrOA-2 (yellow dots). The right maps show the location of the estuarine zone of the Patos Lagoon (upper) and the Rio Grande do Sul State (bottom), both marked as red rectangles.....**29**

**Figure 2.** Means ( $\pm$  standard error) and two-way ANOVA results for six parameters of the carbonate system: (a) salinity, (b) pH at total scale, (c) total alkalinity (TA), (d) state aragonite saturation ( $\Omega_{Ar}$ ), (e) partial pressure of carbon dioxide ( $pCO_2$ ), (f) buffer capacity of pH to fractional change of dissolved inorganic carbon ( $\beta DIC$ ), recorded seasonally for 2 monitoring stations (BrOA-1 and BrOA-2) in the lower zone of Patos Lagoon Estuary. Different letters indicate significant differences between the seasonality within stations, at  $p < 0.05$  with Tukey's tests following post-ANOVA. Note, for instance, the salinity in (a) did not show seasonal differences in the BrOA-2, in opposition to BrOA-1 where the summer differed significantly from both winter and spring. ....**38**

**Figure 3.** Means ( $\pm$  standard error) and two-way ANOVA results for 5 parameters of the carbonate system: (a) total alkalinity (TA), (b) pH at total scale, (c) state aragonite saturation ( $\Omega_{Ar}$ ), (d) partial pressure of carbon dioxide ( $pCO_2$ ), (e) buffer capacity of pH to fractional change of dissolved inorganic carbon ( $\beta DIC$ ), recorded for each range of salinity (low: 0-10, medium: 11-25, high>25) in the 2 monitoring stations (BrOA-1 and BrOA-2) in the lower zone of

Patos Lagoon Estuary. Different letters indicate significant differences between the salinity ranges within stations at  $p < 0.05$  with Tukey's tests following post-ANOVA. Capital letters show significant differences between stations in the same salinity range. Note, for instance, the pH (a) showed differences between low and high salinities in BrOA-2, in opposition to BrOA-1 where the low differed significantly from medium and high salinities.....**39**

**Figure 4.** Distribution of the buffer capacity of pH to fractional change of DIC ( $\beta$ DIC) in relation to salinity and  $\Omega$ Ar (color bar) in the BrOA-1 (diamond) and BrOA-2 (circle) stations in the lower zone of Patos Lagoon Estuary. The dotted lines correspond to the  $\beta$ DIC estimated to riverine endmember ( $\beta$ DIC<sub>riverine</sub> = 38  $\mu$ mol kg<sup>-1</sup>; red dashed line), station means ( $\beta$ DIC<sub>BrOA-1</sub> = 95  $\mu$ mol kg<sup>-1</sup> and  $\beta$ DIC<sub>BrOA-2</sub> = 105  $\mu$ mol kg<sup>-1</sup>; black dashed lines) and ocean endmember ( $\beta$ DIC<sub>ocean</sub> = 212  $\mu$ mol kg<sup>-1</sup>; blue dashed line). The arrows and ellipses indicate the values closest to the saturation threshold for each station.....**41**

**Figure 5.** Monthly variability of pH at total scale in the BrOA-1 (A) and BrOA-2 (B) stations of the lower zone of Patos Lagoon Estuary. Monthly variability of the salinity and chlorophyll-a associated with the buffer capacity of pH to fractional change of dissolved inorganic carbon ( $\beta$ DIC) in the BrOA-1 (C) and BrOA-2 (D) stations. The dotted lines correspond to the mean estimated to pH (pH<sub>BrOA-1</sub> = 7.7 and pH<sub>BrOA-2</sub> = 7.83; black dashed line), and  $\beta$ DIC to both stations ( $\beta$ DIC<sub>BrOA-1</sub> = 95  $\mu$ mol kg<sup>-1</sup> and  $\beta$ DIC<sub>BrOA-2</sub> = 105  $\mu$ mol kg<sup>-1</sup>; red dashed lines).....**43**

**Figure 6.** Seasonal effect of temperature, salinity, dissolved inorganic carbon (DIC), and total alkalinity (TA) on surface pH for BrOA-1 (A) and BrOA-2 (B) stations in the lower zone of Patos Lagoon Estuary. The error bar (purple) accompanied by its numerical value shows the difference between the current pH variation and the sum of all the drivers.....**46**

**Figure 7.** Schematic representation of the seasonal variability of the buffering capacity in the lower zone of Patos Lagoon Estuary. The means of the state of aragonite saturation ( $\Omega$ Ar), buffering capacity of pH ( $\beta$ DIC), and pH are

displayed upper of the seasonal means of  $\beta$ DIC at summer (sun), autumn (leaves), winter (ice crystal), and spring (flowers). The colors utilized (blue and grey) emphasize spatial discrepancies in pH and seasonal variations in  $\beta$ DIC at the inner station BrOA-1. The salinity gradient color and dotted arrows represent the seasonal influence of the freshwater (brown to yellow) and seawater (blue to green) endmembers in the inner (BrOA-1) and outer (BrOA-2) environments of the studied region.....53

**Figure S.1.** Rate of change or sensitivity factor of  $p\text{CO}_2$  (a), pH (b), and  $\text{CO}_3^{2-}$  (c) per DIC unit throughout the salinity gradient at the BrOA-1 (yellow) and BrOA-2 (blue) stations in the lower zone of Patos Lagoon Estuary. Each sensitivity factor graphic displays the scattering of its data points along its fit using a weighted least squares regression accompanied by confidence bands for each station.....58

**Figure S.2.** Seasonal variation of temperature ( $^{\circ}\text{C}$ ), salinity, total alkalinity ( $\mu\text{mol kg}^{-1}$ ), and dissolved inorganic carbon ( $\mu\text{mol kg}^{-1}$ ) relative to their annual means.....59

## **CAPÍTULO VI**

Figura 1. Representação esquemática da variabilidade sazonal da capacidade tampão no baixo Estuário da lagoa dos Patos. As médias do estado de saturação da aragonita ( $\Omega_{\text{Ar}}$ ), capacidade tampão do pH ( $\beta$ DIC) e pH são exibidas acima das médias sazonais de  $\beta$ DIC no verão (sol), outono (folhas), inverno (cristal de gelo) e primavera (flores). As cores utilizadas (azul e cinza) enfatizam as discrepâncias espaciais no pH e as variações sazonais no  $\beta$ DIC na estação interna BrOA-1. A cor do gradiente de salinidade e as setas pontilhadas representam a influência sazonal dos membros finais de água doce (marrom a amarelo) e água do mar (azul a verde) nos ambientes interno (BrOA-1) e externo (BrOA-2) da região estudada.....62

# Lista de Tabelas

## CAPÍTULO V

**Table 1.** Maximum estuarine acidification (MEA) salinity estimates derived from the intersection of  $\text{CO}_2$  and  $\text{CO}_3^{2-}$  concentrations as a function of the salinity for BrOA-1 and BrOA-2 stations in the lower zone of Patos Lagoon Estuary.....**45**

**Table 2.** Buffer capacity of pH to fractional change of dissolved inorganic carbon ( $\beta\text{DIC}$ ) in coastal ecosystems and ocean. The table displays the mean or range report of salinity, total alkalinity (TA), pH at total scale, state of aragonite saturation ( $\Omega\text{Ar}$ ), partial pressure of carbon dioxide ( $p\text{CO}_2$ ), dissolved inorganic carbon (DIC), and  $\beta\text{DIC}$ . BrOA-1 and BrOA-2 represent, respectively, the conditions at the inner and outer zones of the Patos Lagoon Estuary (PLE).....**50**

**Table S.1.** Mean and standard error of the propagated uncertainties in the calculation of the carbon dioxide system in the lower estuary for each season. The unit of each uncertainty corresponds to the unit of each evaluated variable: DIC ( $\mu\text{mol kg}^{-1}$ ),  $p\text{CO}_2$  ( $\mu\text{atm}$ ),  $\Omega\text{Ar}$  (unitless),  $\text{CO}_2$  ( $\mu\text{mol kg}^{-1}$ ),  $\text{CO}_3^{2-}$  ( $\mu\text{mol kg}^{-1}$ ).....**55**

**Table S.2.** Means ( $\pm$  standard error) and two-way ANOVA results for six parameters of the carbonate system (salinity, TA, pH,  $\Omega\text{Ar}$ ,  $p\text{CO}_2$ ,  $\beta\text{DIC}$ ) recorded seasonally at two monitoring stations (BrOA-1 and BrOA-2) in the lower estuary of Patos Lagoon. Results of two-way ANOVA are displayed in the third set of lines. Asterisks indicate significance of ANOVA (\* =  $p < 0.05$ , \*\* =  $p < 0.01$ , \*\*\* =  $p < 0.001$ , ns: non-significant). Different letters indicate significant differences ( $p < 0.05$ ) between the seasons within stations, evaluated with post-ANOVA Tukey's tests at a significance level of  $p < 0.05$ . Lowercase letters denote seasonal means and capital letters represent station means.....**56**

**Table S.3.** Mean values ( $\pm$  standard error) and results of two-way ANOVA for five parameters of carbonate system (pH, TA,  $\Omega\text{Ar}$ ,  $p\text{CO}_2$ ,  $\beta\text{DIC}$ ) recorded within

different salinity ranges at two monitoring stations (BrOA-1<sub>inner</sub> and BrOA-2<sub>outer</sub>) in the lower zone of Patos Lagoon Estuary. Results of two-way ANOVA are displayed in the third set of lines. Asterisks indicate significance of ANOVA (\* =  $p < 0.05$ , \*\* =  $p < 0.01$ , \*\*\* =  $p < 0.001$ , ns: non-significant). Different lowercase letters indicate significant differences ( $p < 0.05$ ) between salinity ranges within the stations (low: 0-10, medium: 11-25, and high: >25), evaluated with Tukey's post-ANOVA tests at a significance level of  $p < 0.05$ . Lowercase letters denote range salinity means and capital letters represent station means.....**57**

**Table S.4.** Constant effect or sensitivity factor of the temperature, salinity, DIC, and TA on pH.....**57**

# Lista de Acrônimos e Abreviações

## B

**BR-LTER:** *Brazilian Long Term Ecological Research*; Pesquisa Ecológica Brasileira de Longa Duração

## C

**Chl-a:** *Chlorophyll a*; Clorofila-a

## D

**DIC:** *Dissolved inorganic carbon*; carbono inorgânico dissolvido

## M

**MEA:** *Maximum estuarine acidification*; máxima acidificação estuarina

## P

**ppb:** *Parts per billion*; partes por bilhão

**PLE:** *Patos lagoon estuary*; estuário da lagoa dos Patos

**pH<sub>Total</sub>** : *pH at total scale*; pH em escala total

## R

**RJ:** Estado do Rio de Janeiro

**RS:** Estado do Rio Grande do Sul

## S

**SF $\Omega$ :** *Sensitivity factor of CO<sub>3</sub><sup>2-</sup> in terms of fractional change per unit change of DIC*; Fator de sensibilidade do CO<sub>3</sub><sup>2-</sup> em termos de alteração fracional por unidade de alteração de DIC

**SF $\beta$ :** *Sensitivity factor of pH in terms of fractional change per unit change of DIC*; Fator de sensibilidade do pH em termos de alteração fracional por unidade de alteração de DIC

**SF $\gamma$ :** *Sensitivity factor of pCO<sub>2</sub> in terms of fractional change per unit change of DIC*; Fator de sensibilidade do pCO<sub>2</sub> em termos de alteração fracional por unidade de alteração de DIC

**S:** *Surface salinity*, salinidade da superfície da água.

## T

**T:** *Surface temperature*, temperatura da superfície da água.

**TA:** *Total alkalinity*; alcalinidade total.

## Grego

**$\beta_{pH}$ :** *Buffer capacity of pH*; Capacidade tampão do pH.

**$\Omega_{Ar}$ :** *State of aragonite saturation*, estado de saturação da aragonita.

**$\Delta X$ :** *annual mean*; média anual.

# Resumo

Estudos precedentes mostraram que os ecossistemas costeiros estão experimentando uma ampla variação de pH entre -0,023 a 0,023 unidades de pH por ano, sendo suscetíveis principalmente a condições de acidificação ou basificação. Essa variabilidade está predominantemente associada ao metabolismo dos ecossistemas e à influência dos ambientes oceânicos e fluviais, como ocorre no sistema subtropical do estuário da Lagoa dos Patos (PLE, sul do Brasil), cuja variabilidade biogeoquímica é governada principalmente por processos de dissolução e concentração de sais. Este estudo analisou e quantificou, pela primeira vez, as mudanças sazonais do tamponamento do pH nas zonas interna e externa do PLE através de diferentes abordagens: (i) a variabilidade temporal dos parâmetros do sistema carbonato, (ii) o fator de sensibilidade do parâmetro (taxa de mudança de um componente específico do sistema de carbonato pela alteração de outro), (iii) a capacidade tampão do pH para mudança fracionária de carbono inorgânico dissolvido ( $\beta$ DIC), (iv) a salinidade máxima da acidificação estuarina (MEA) e (v) os parâmetros controladores ou *drivers* sazonais de pH (temperatura, salinidade, DIC e alcalinidade total – TA). Um monitoramento superficial da TA, pH e parâmetros físico-químicos foi realizado de maio de 2017 a novembro de 2022.  $\beta$ DIC e outras variáveis do sistema de carbonato foram estimadas usando o pacote Seacarb do software R e a ferramenta macro do Excel CO<sub>2</sub>Sys. Os resultados não mostraram disparidade sazonal no pH e  $\beta$ DIC na zona externa, ao contrário da zona interna que registou uma variabilidade significativa principalmente entre verão e inverno. Durante o inverno, houve uma dissolução predominante de CaCO<sub>3</sub> devido ao aporte fluvial com baixo tamponamento. No entanto, a zona interna apresentou um maior  $\beta$ DIC em baixa salinidade associada a seu valor mais alto da salinidade de máxima acidificação estuarina (MEA), onde o efeito das adições de CO<sub>2</sub> no pH diminui à medida que se afasta da salinidade da MEA. A dinâmica mensal do  $\beta$ DIC em ambas zonas esteve principalmente relacionada com a variabilidade da salinidade, com influência predominante de janeiro a julho, enquanto a influência da variabilidade da clorofila-a prevaleceu durante os meses de alta descarga de água. O influxo de

água doce determinou a disparidade sazonal da influência de cada *driver* ambiental na variabilidade do pH. Um efeito uniforme de cada *driver* foi observado no outono, em contraste com o verão, quando a mudança de pH foi associada principalmente ao efeito negativo do aumento da DIC, regulado pelo aumento da TA. As condições de subsaturação da aragonita em salinidade média e alta suportam a premissa de uma capacidade tampão moderada-baixa no baixo estuário da lagoa Dos Patos.

**Palavras-chave:** Capacidade tampão, Acidificação estuarina, Ambiente costeiro, lagoa dos Patos.

# Abstract

Earlier studies showed that coastal ecosystems undergo a broad pH trend from  $-0.023$  to  $0.023$  pH units  $\text{yr}^{-1}$ , being susceptible mainly to acidification or basification conditions. This range is predominantly associated with ecosystem metabolism and the influence of ocean and riverine endmembers, as has been observed in the subtropical system of the Patos Lagoon Estuary (PLE, south Brazil), whose biogeochemical variability is mainly governed by processes of dissolution and concentration of salts. This study analyzed and quantified for the first time the seasonal changes of pH buffering in the inner and outer zones of the PLE through the evaluation of different approaches: (i) the temporal variability of the carbonate system parameters, (ii) the parameter sensitivity factor (i.e., the rate of change of a specific component of the carbonate system by the alteration of another), (iii) the buffering capacity of pH to fractional change of dissolved inorganic carbon ( $\beta\text{DIC}$ ), (iv) the maximum estuarine acidification (MEA) salinity and (v) the seasonal drivers of pH (i.e., temperature, salinity, DIC and total alkalinity – TA). A surface monitoring of TA, pH, and physical-chemical parameters was performed and evaluated from May 2017 to November 2022.  $\beta\text{DIC}$  and other carbonate system variables were estimated using the package *seacarb* of R software and the  $\text{CO}_2\text{Sys}$  Excel macro tool. The results did not show a seasonal disparity in the pH and its  $\beta\text{DIC}$  in the outer zone, unlike the inner zone which recorded significant variability mainly between summer and winter. During winter, there was a predominant  $\text{CaCO}_3$  dissolution by a river input with low buffering. Despite that, the inner zone recorded the higher buffering in low salinity associated with its higher MEA

salinity, where the effect of CO<sub>2</sub> additions on pH decreases at salinities lower than this equilibrium point. The monthly dynamic of βDIC in both zones was mainly related to the variability of salinity with predominant influences from January to July, while the influences of the variability of chlorophyll-a prevailed during months of high-water discharge afterward. The freshwater discharge determined the seasonal disparity of the influence of each environmental driver on pH variability. A uniform effect of each driver was observed in autumn, in contrast to summer when pH change was associated mainly with the negative effect of increased DIC, regulated by the increase in TA. The aragonite undersaturation conditions in medium and high salinity supported the premise of a moderate-low buffering capacity in the lower zone of the PLE.

**Keywords:** Buffering capacity, coastal acidification, coastal ecosystems, biogeochemical dynamics.

# Capítulo I: Introdução

As mudanças de acidez nos oceanos, equivalente a 0,1 unidade de pH (30% de aumento) desde a etapa industrial, foram inequivocamente associadas ao incremento nas concentrações de gases de efeito estufa causado pelas atividades humanas. Em 2019, as concentrações médias eram de 410 parte por milhão de dióxido de carbono, 1866 parte por bilhão (ppb) de metano e 322 ppb de óxido nitroso em 2019 [IPCC, 2021]. A tendência decrescente de pH entre  $-0,0004$  e  $-0,0026$  unidades de pH ano por ano, observada entre 1989 e 2014, contrasta com a variação não uniforme reportada nos ecossistemas costeiros ( $-0,023$  a  $0,023$  unidades de pH por ano). Esses ecossistemas experimentam tendências que variam desde acidificação até basificação [Carstensen & Duarte, 2019]. A variação do pH nos ecossistemas costeiros tem sido associada principalmente à influência e interação dos *endmembers*, assim como aos processos metabólicos nas zonas de mistura e interfaces. Esses processos desempenham um papel significativo na dinâmica biogeoquímica, resultando em um aumento ou diminuição do pH, dependendo do tempo de residência [Regnier et al., 2013, Duarte et al., 2013, Cai et al., 2021]. A análise das tendências e fontes de variabilidade no ecossistemas costeiros, conforme apresentada por Carstensen & Duarte [2019] resumiu, de maneira

conceitual, os componentes reguladores do pH: (I) a extensão de águas costeiras tamponadas derivadas da TA fornecida pelo rio, (II) a extensão da mistura com água oceânica, e (III) o balanço do metabolismo ecossistêmico pela adição e remoção do carbono inorgânico dissolvido (DIC).

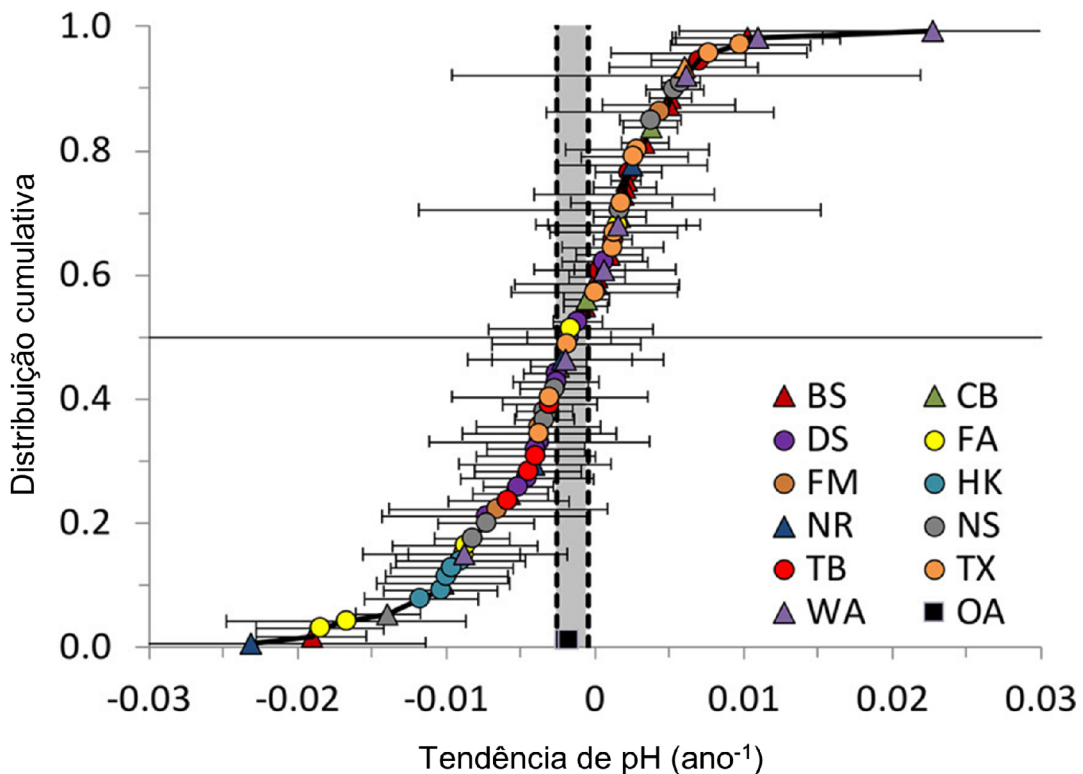


Figura 1. Distribuição cumulativa de decréscimo nas tendências do pH em 83 sistemas costeiros, em comparação com decréscimos nas estações dos projetos de Estudo de Séries Temporais Atlântico das Bermudas (BATS) e Oceano de Hawaii (HOT) (acidificação do oceano - OA), e a gama de decréscimos oceânicos reportados na literatura (linhas tracejadas). Sistemas costeiros com baixo tamponamento são marcados com triângulos. As barras de erro mostram o intervalo de confiança de 95% das reduções de pH costeiras estimadas. Observe que as barras de erro OA são menores que os símbolos. Figura modificada de Carstensen & Duarte [2019].

Os estuários, com apenas 0,3% da água superficial global, são sistemas inerentemente dinâmicos considerados entre os mais produtivos, atuando como filtradores ou exportadores de nutrientes e matéria orgânica para as áreas costeiras adjacentes [Cai, 2011]. O impacto dos processos

antropogênicos, associados ao desenvolvimento urbano e diversificação de atividades nestas áreas, levou a uma mistura sem precedente do estresse antropogênico e climático, com efeitos que podem alterar sua capacidade tampão. Isso foi verificado no aumento da TA nos rios estadunidenses de Delaware (400-900  $\mu\text{mol kg}^{-1}$ ) e Mississippi (1400-2800  $\mu\text{mol kg}^{-1}$ ), e nos rios suecos (300-460  $\mu\text{mol kg}^{-1}$ ), nos últimos 50-100 anos (Fig.2), associado ao intemperismo das rochas carbonatadas e ao uso de cal na agricultura, sendo subsequentemente exportado para áreas costeiras adjacentes [Duarte et al 2013].

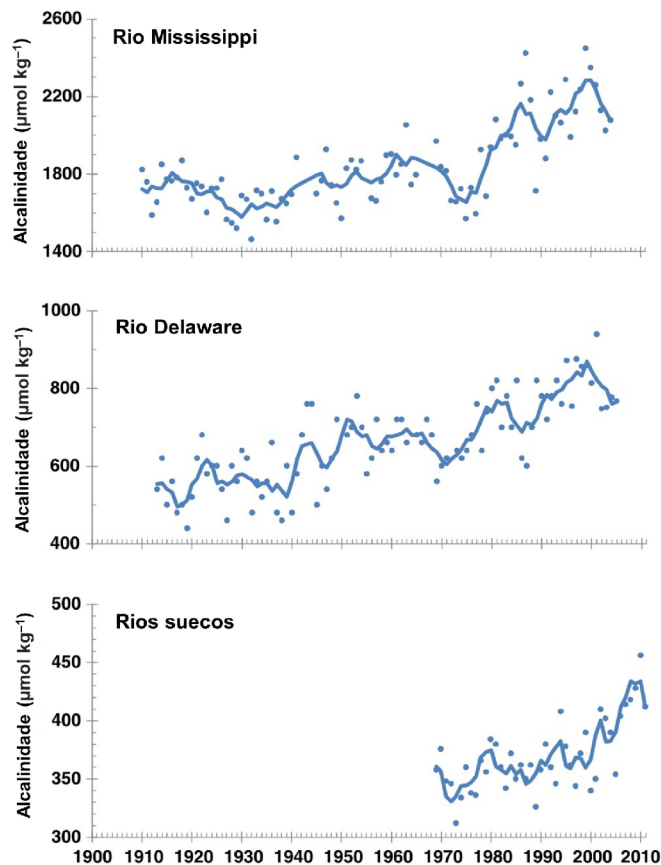


Figura 2. Séries temporais de alcalinidade nos rios estadunidenses Mississippi (a), rio Delaware (b) e rios suecos (c). As linhas sólidas representam uma média móvel de 5 anos das concentrações médias anuais. Figura modificada de Duarte et al [2013].

O estuário Kemi (Finlândia) apresentou flutuações interanuais entre 1980-2017, com uma tendência de incremento do pH (7,1-7,4) em um ambiente salino e de baixo tamponamento. Essa condição tampão foi mais associada com as variações de salinidade do que com a baixa e relativamente uniforme atividade biológica. No estuário de Westerschelde (Países Baixos), a alta entrada de matéria orgânica na década de 1970, gerou um acentuado estado heterotrófico, com um pH de 7,63. Posteriormente, com a redução de mais de 50% do aporte de nitrogênio total, foi registrado um pH de 7,87 em 2014; um aumento não tão pronunciado devido a sua elevada capacidade tampão (TA de 4000  $\mu\text{mol kg}^{-1}$ , salinidade < 2) [Hellings et al. 2013]. A extensão espacial e temporal dos processos ou fatores forçantes da variabilidade do pH pode induzir condições de acidez, com baixos pH e estado de saturação do aragonita ( $\Omega_{\text{Ar}}$ ), reduzindo a capacidade tampão e aumentando a exposição e magnitude das condições corrosivas ( $\Omega_{\text{Ar}} < 1$ ). Isso ocorreu no final do verão no mar de Salish, no noroeste do Oceano Pacífico, onde a remineralização da matéria orgânica, juntamente com ventos relativamente fracos e estratificação em algumas áreas, forçou uma diminuição no pH e  $\Omega_{\text{Ar}}$  [Bednaršek et al., 2021].

Os estuários das regiões norte e nordeste do Brasil registraram uma ampla faixa de TA, entre 131 e 2800  $\mu\text{mol L}^{-1}$  (1298  $\mu\text{mol L}^{-1}$ ), e um pH oscilando entre 6,6 e 8,2. A alta correlação negativa entre a porcentagem de saturação do oxigênio dissolvido e a  $p\text{CO}_2$  foi atribuída a uma intensa decomposição de matéria orgânica na água de fundo e/ou sedimento, resultando na diminuição do pH nesses sistemas estuarinos [Noriega et al., 2014]. Nas águas costeiras eutróficas da baía de Guanabara (RJ), o metabolismo ecossistêmico foi o principal controle da variação espaço-temporal do estado de saturação da

aragonita, com episódios de condições mais corrosivas em águas pobremente tamponadas que receberam diretamente descargas de efluentes domésticos e rios poluídos. Em contraste, valores elevados foram registrados nas águas estratificadas médias superiores, dominadas pelas florações fitoplanctônicas e com alta capacidade de tamponamento [Cotovicz et al., 2017]. Um diferente cenário foi observado no estuário oligotrófico de São Francisco (entre os estados de Sergipe e Alagoas), no qual as águas com baixo tempo de residência, quentes e com baixo tamponamento do pH, promoveram a predominância do equilíbrio termodinâmico do sistema carbonato sobre os processos biológicos, determinando os fluxos de  $\text{CO}_2$  na interface ar-água nos processos de misturas [Abril et al., 2021]. Na laguna costeira cálida e hipersalina de Araruama (RJ), as florações fitoplanctônicas, os altos valores de pH, a alta capacidade de tamponamento e o aumento do metabolismo autotrófico e da  $p\text{CO}_2$  (decorrente da precipitação do  $\text{CaCO}_3$ ), geraram um sumidouro líquido anual de  $\text{CO}_2$ . Os valores altos de  $p\text{CO}_2$  no verão em relação ao inverno, estiveram associados com os efeitos termodinâmicos causados pelo aquecimento das águas e aumento da salinidade [Cotovicz et al., 2021].

O baixo PLE (região sul do Brasil) apresentou um ambiente alcalino nas águas superficiais, com um pH médio de 8 e supersaturação de  $\text{CaCO}_3$ . No entanto, condições de subsaturação da calcita foram registadas para os meses de enchente, com uma menor extensão temporal que  $\Omega_{\text{Ar}}$ . Neste sistema os processos de diluição (associado à entrada água doce) e concentração de sais (intrusão salina não associado aos processos que mudam o estado da água) foram os principais mecanismos responsáveis para as mudanças dos parâmetros do sistema de carbonato nas águas superficiais [Albuquerque et al,

2022] (Fig. 5). Adicionalmente, uma variação sazonal significativa nos fluxos água-ar de  $\text{CO}_2$  foi identificada associada com os padrões sazonal de influxo de água doce marcando períodos tanto de absorção (Dezembro e Maio) quanto de degaseificação de  $\text{CO}_2$  (Junho e Novembro), principalmente no interior do baixo estuário [Albuquerque et al., 2023]. A avaliação diária do metabolismo ecossistêmico pelágico no canal do estuário determinou condições predominantes heterotróficas para o verão do 2021, com clara evidência da intrusão da pluma do rio da Prata, possivelmente representando um importante factor na biogeoquímica local [Bordin et al., 2023].

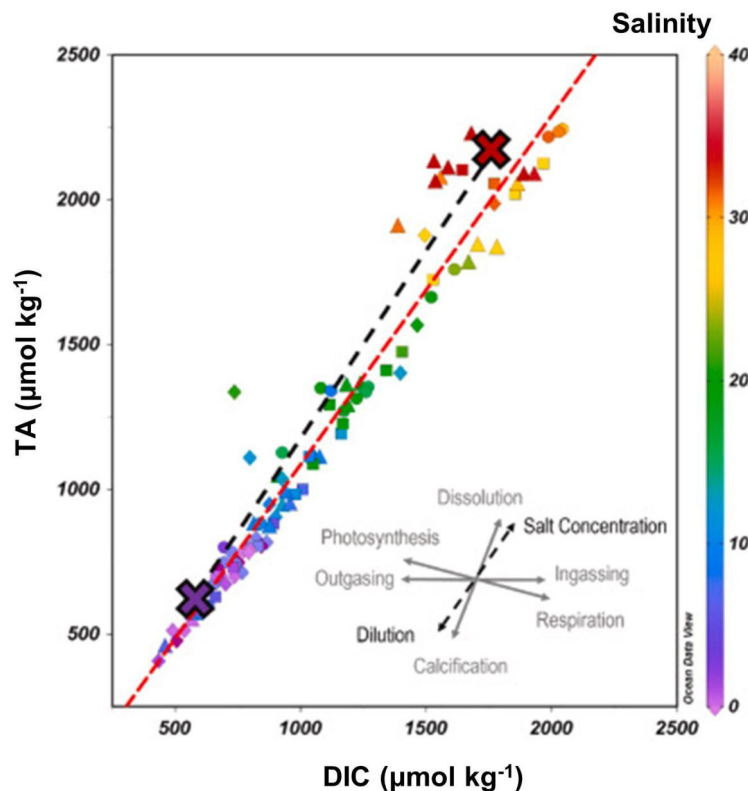


Figura 3. Diagrama de dispersão da alcalinidade total (TA;  $\mu\text{mol kg}^{-1}$ ) e do carbono inorgânico total dissolvido (DIC;  $\mu\text{mol kg}^{-1}$ ). O diagrama TA-DIC-salinidade considerou o conjunto de dados da rede BrOA, abrangendo entre maio de 2017 e junho de 2021, com o verão representado por pontos, o outono por triângulos, o inverno por quadrados e a primavera por losangos. As setas inseridas mostram os principais processos (conforme indicado), adaptados de Zeebe e Wolf-Gladrow (2007), que regem a variabilidade no sistema carbonato do estuário da lagoa dos Patos. A linha preta tracejada representa a linha de mistura conservativa teórica de águas fluviais e oceânicas que indicam o efeito da diluição e concentração de sal na mudança das concentrações de TA-DIC. As cruzes roxa e vermelha representam os membros

extremos das águas fluviais e oceânicas. A linha tracejada vermelha representa a curva de regressão linear do conjunto de dados. Figura modificada de Albuquerque et al. [2022].

Os estudos mencionados basearam-se na análise temporal das variáveis do sistema carbonato (pH,  $\Omega_{Ar}$ , TA) para inferir a capacidade de tamponamento ou determinar o efeito da acidificação na biocalcificação [Li et al., 2020]. No entanto, essas variáveis não quantificam a sensibilidade ou tamponamento do sistema (resistência) sob a pressão de um parâmetro controlador ao longo de um gradiente de salinidade. O fator Revelle (Equação 1) é comumente usado para quantificar a sensibilidade da  $pCO_2$  às adições de DIC, porém não explica a alteração do pH [Hu et al., 2013; Middelburg et al., 2020; Cai et al., 2020].

$$\text{Fator Revelle} \approx (3TA \times DIC - 2DIC) / ((2DIC - TA) (TA - DIC)) \dots \dots \dots 1$$

O presente estudo teve como objetivo determinar e quantificar a sensibilidade e a capacidade tampão do pH frente às mudanças sazonais nas estações de monitoramento localizadas no interior e exterior do baixo PLE. O fator  $\beta_{DIC}$  proposto por Egleston et al. [2020] foi usado como uma medida direta da resposta do pH às adições de DIC, simultaneamente e complementar à análise sazonal das variáveis do sistema de carbonato. Além disso, o efeito dos *drivers* ambientais sobre o pH foi estimado para inferir os processos ou fatores responsáveis por sua variabilidade sazonal. Este estudo não apenas representa uma contribuição significativa ao avanço do conhecimento observacional e metodológico do pH em sistemas estuarinos subtropicais do Hemisfério Sul, como também serve como um catalisador para futuras pesquisas. Entre as áreas que merecem especial atenção está a determinação do limite de saturação de  $CaCO_3$  dos organismos calcificadores presentes nesse ecossistema. Além disso, a pesquisa incentiva a identificação de áreas

que oferecem condições ideais de tamponamento contra as mudanças sazonais de pH. Essas investigações não apenas têm o potencial de minimizar os efeitos dessa variabilidade nos recursos vivos, mas também fornecem conhecimentos fundamentais para o desenvolvimento sustentável da aquicultura, sendo assim essenciais para orientar as práticas futuras neste campo.

## Capítulo II: Objetivos

A fim de alcançar uma maior compreensão da dinâmica sazonal da capacidade tampão do pH na região do baixo PLE, os seguintes objetivos foram levantados neste estudo.

### **Objetivo geral**

Investigar a capacidade do tamponamento do pH no sul do estuário da lagoa dos Patos.

### **Objetivos específicos**

- Descrever as variações sazonais do pH na água de superfície;
- Identificar e determinar as principais variáveis controladores e os processos associados que alteram o pH da água;
- Determinar a capacidade de tamponamento do estuário e sua relação com as variáveis controladores do pH.

## Capítulo III: Área de estudo

A lagoa dos Patos é a maior lagoa costeira do Brasil e do mundo. A lagoa está localizada entre as latitudes 30°S e 32°S no estado do Rio Grande do Sul (RS), abrangendo uma área de 10,360 km<sup>2</sup> com uma bacia hidrográfica de aproximadamente 200.000 km<sup>2</sup> ligada ao Oceano Atlântico Sul através de um canal na cidade de Rio Grande [Seeliger, 2001; Lemke et al., 2007]. O ecossistema é classificado como uma lagoa costeira rasa, com profundidade média de 5 a 6 m. Este sistema tem uma orientação NE-SW, paralela à linha de costa do RS e à direção predominante do vento, sendo este último a principal força que influencia seu regime hidrodinâmico, e uma amplitude de maré astronômica de 0,45 m [Marinho et al., 2020]. A distribuição da lagoa abrange regiões subtropicais e temperadas quentes, com uma temperatura média do ar de 18 °C, uma precipitação máxima anual que oscila entre 1200 e 1500 mm [Abreu et al., 2016] e uma descarga fluvial anual média de cerca de 2400 m<sup>3</sup>s<sup>-1</sup> [Andrade et al., 2022].

O período final do inverno e a estação da primavera registram as maiores descargas de água doce, enquanto o outono apresenta a menor e a maior intrusão de água do mar, resultando em inundação e salinização do PLE

[Möller et al., 2001]. Essa intrusão de água salina é limitada ao baixo estuário, que representa 10% da área total da lagoa, produzindo um amplo gradiente de salinidade de 0 a 35 [Seeliger, 2001; Vaz et al., 2006]. Em termos tróficos, o canal central no baixo estuário apresenta predominantemente uma condição equilibrada, classificada como mesotrófica. Isso se deve à sua elevada capacidade de autodepuração por diluição, que é facilitada pela maior hidrodinâmica e menor tempo de residência das massas de água no canal [Baumgarten et al., 2013]. Em relação aos processos biogeoquímicos, a variabilidade dos parâmetros do sistema carbonato é principalmente influenciada pela diluição e concentração de sais. Estes processos, definidos pelos seus padrões hidrológicos, sugerem dois cenários biogeoquímicos distintos no estuário: (I) dominância oceânica durante o verão e outono, e (II) dominância fluvial durante o inverno e a primavera. O último cenário apresenta maior suscetibilidade a condições de subsaturação [Albuquerque et al., 2022].

Apesar do tempo de troca de água entre a lagoa dos Patos e o oceano Atlântico ser de aproximadamente dois dias [Gordey e Osadchiev, 2022], o baixo estuário apresenta uma disparidade entre suas zonas. A foz do estuário (zona externa) está sujeita a correntes fortes, com um tempo de residência ligeiramente mais curto em comparação com a zona interna somera, com sua circulação parcialmente restrita [Albuquerque et al., 2022]. Essas diferenças se refletem nas variações consideráveis na concentração e composição do fitoplâncton, provavelmente associadas às distintas condições hidrológicas [Abreu et al., 2016]. As duas zonas abrigam duas estações de monitoramento contínuo (Fig. 1) do programa Rede Brasileira de Acidificação dos Oceanos [BrOA Network; [www.broa.furg.br](http://www.broa.furg.br); Kerr et al., 2016] e da Pesquisa Ecológica

Brasileira de Longa Duração (BR-LTER) do programa PLE e Costa Marinha Adjacente [www.peld.furg.br; Odebrecht and Abreu, 2019]. A primeira estação (BrOA-1) está localizada numa enseada interna. Sua profundidade rasa (< 2 m) e baixo regime hidrodinâmico fazem do vento a principal força que estimula a mistura da coluna da água e a troca com os sedimentos de fundo. Além disso, esta estação está predisposta à influência de esgoto industrial e doméstico da cidade de Rio Grande. A segunda estação (BrOA-2) está localizada perto da foz do estuário, em uma zona exterior inferior. Sua maior profundidade (~12 m) e a maior influência das intrusões do oceano Atlântico Sul e do vento favorecem a formação de estruturas verticais de salinidade que oscilam desde uma cunha salina até um gradiente bem misturado [Möller et al., 2001].

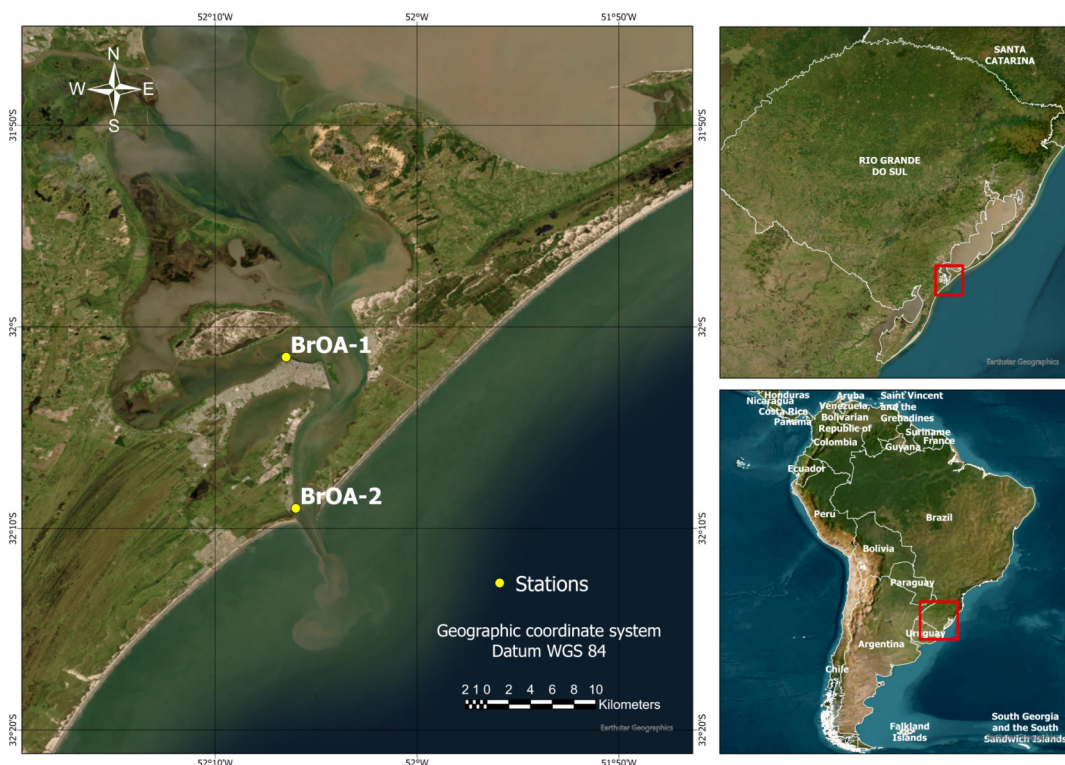


Figura 1. Mapa da zona estuarina inferior do Estuário da Lagoa dos Patos (esquerda) com localização das estações de monitoramento fixas no cais BrOA-1 e BrOA-2 (pontos amarelos). Os mapas da direita mostram a localização da zona estuarina da Lagoa dos Patos (parte superior) e do Estado do Rio Grande do Sul (parte inferior), ambas marcadas como retângulos vermelhos.

# Capítulo IV: Material e Métodos

## **Amostragem e procedimentos analíticos**

A base de dados faz parte de dois grandes programas de monitoramento, rede BrOA (iniciado em outubro de 2015) e LTER-PLE, este último com o maior conjunto de dados temporais (desde 1998) sobre a biota estuarina e marinha e variáveis abióticas no Hemisfério Sul [Lemos et al ., 2022]. Os dados, com frequência mensal para o período de maio de 2017 a novembro de 2022, incluem as seguintes variáveis: temperatura, salinidade, concentrações de nutrientes inorgânicos dissolvidos e de clorofila-*a* (Chl-*a*) do programa LTER-PLE, além de TA e pH do programa BrOA. Em ambos os programas, os parâmetros foram obtidos e medidos a partir de amostras de água coletadas com uma garrafa Van Dorn de 5 L a uma profundidade de 1 m abaixo da superfície, nas estações fixas localizadas nas zonas interna e externa (Fig.1) do baixo estuário.

## **Temperatura, salinidade, nutrientes e clorofila-*a***

A temperatura e a salinidade foram medidas in situ utilizando um termômetro digital e um refratômetro óptico YSI modelo 33 SCT, respectivamente, sendo este último verificado em laboratório com um medidor de condutividade

Metrohm® 914. As amostras para análise de nutrientes inorgânicos e de Chl-a foram coletadas em frascos plásticos e preservadas em câmara frigorífica para posterior análise em laboratório. As concentrações dos nutrientes inorgânicos (ácido silícico, fosfato, nitrito e nitrato) foram analisados em amostras filtradas através de filtros de membrana de acetato de celulose, com um SEAL Analytical Autoanalyzer AA3 HR de acordo com a metodologia descrita por Grasshoff et al. (2009). A concentração de Chl-a foi determinada filtrando uma alíquota de 50–250 mL (dependendo da concentração de material) através de filtros Whatman GF/F sob luz fraca, seguido de congelamento ( $-80^{\circ}\text{C}$ ) para medição posterior usando um fluorímetro calibrado Turner Designs TD-700, com correção para produto de degradação usando o método de não acidificação descrito por Welshmeyer [1994].

### **Alcalinidade total e pH**

As amostras para análise de TA foram coletadas usando frascos de vidro borossilicato de 500 mL [Dickson et al. 2007]. As amostras foram imediatamente fixadas com solução de cloreto de mercúrio para evitar qualquer atividade biológica e posteriormente refrigeradas para evitar a evaporação. As análises em laboratório foram realizadas por titulação potenciométrica de cela fechada [Dickson et al., 2007] usando um titulador automático (Metrohm® Titrand 888) e um eletrodo de referência de vidro combinado (Metrohm® 6.0262.100) a uma temperatura controlada de  $25 \pm 0,1^{\circ}\text{C}$  mantida por banho termostático. Devido à ampla faixa de salinidade do estuário, uma adaptação do método de cela fechada, descrito em Albuquerque et al. [2022], foi adotado. A avaliação diária com réplicas de uma única amostra permitiu avaliar a consistência das

medidas, com uma precisão da análise do TA de  $4 \mu\text{mol kg}^{-1}$ , com um intervalo entre 2,3 e  $5 \mu\text{mol kg}^{-1}$ .

As amostras para a determinação de pH foram coletadas em frascos de borosilicato âmbar de 125 mL e preservadas em caixa térmica de isopor até a medição em laboratório. A medição de cada amostra (no máximo 2 horas após a amostragem) foi efetuada com um sensor de pH Metrohm® 913, ou 914, acoplado a uma célula de eletrodo de referência de vidro e sensor de temperatura, que foram previamente padronizados usando soluções tampão com padrões de pH Fluka® de 4.00 e 7.41, ambos a  $25^{\circ}\text{C}$  até janeiro de 2021 e, posteriormente, Merck® Certipur de 4, 7 e 9, todos a  $20^{\circ}\text{C}$ . A incerteza da determinação foi  $< 0,05$  unidades de pH em escala NBS e os valores foram corrigidos para a temperatura *in situ* pela equação desenvolvida por Gieskes [1969]. A escala total foi escolhida e posteriormente utilizada para o pH à temperatura *in situ*.

### **Processamento de dados e análise estadísticas**

Os parâmetros do sistema carbonato e a conversão da escala de pH foram estimados usando a macro *CO2sys\_v3.0\_err.xlsm* versão 3.0, desenvolvida por Lewis et al. [1998] e modificado por Pierrot et al. [2021], utilizando como parâmetros de entrada a temperatura, salinidade, TA, pH, concentração de ácido silícico e fosfato. Devido à grande variação de salinidade e temperatura, foram escolhidas as constantes de dissociação  $k_1$  e  $k_2$  relatadas por Millero [2010], também utilizadas por Hu et al. [2017], McCutcheon et al. [2019] e McCutcheon e Hu [2022], em sistemas estuarinos. Além disso, foram usadas as constantes de sulfato e borato relatadas por Dickson [1990] e Lee et al. [2010], respectivamente. As incertezas dos parâmetros calculados do sistema

carbonato foram determinadas pelo método relatado por Orr et al. [2018] usando o pacote *seacarb* do software R [Gattuso et al., 2021]. O erro propagado é uma estimativa do erro associado à seleção de variáveis e constantes para o cálculo dos parâmetros do sistema carbonato. As variáveis estimadas apresentaram as seguintes incertezas (médias e erros padrão): DIC:  $14 \pm 0,7 \mu\text{mol kg}^{-1}$ ,  $p\text{CO}_2$ :  $75 \pm 3 \mu\text{atm}$ ,  $\Omega\text{Ar}$ :  $0,10 \pm 0,007$ ,  $\Omega\text{Ca}$ :  $0,17 \pm 0,012$ ,  $\text{CO}_2$ :  $2,9 \pm 0,12 \mu\text{mol kg}^{-1}$  and  $\text{CO}_3^{2-}$ :  $6,7 \pm 0,50 \mu\text{mol kg}^{-1}$ . Na conversão da escala de pH, o pH na escala total registrou uma diferença média de 0,142 unidades menor que a escala NBS, valor não muito distante do descrito no macro que estima um resíduo de 0,13 em condições de salinidade de 20, temperatura de 25°C e pressão de 1 atm.

A estatística descritiva, testes de normalidade e transformação de *Box-Cox* foram realizadas para identificar *outliers* e atender os pressupostos paramétricos usando software R (version 4.2.2, 2022). Para estabelecer a variação temporal e/ou espacial da capacidade de tamponamento, uma ANOVA de duas vias dos parâmetros do sistema de carbonatos foi desenvolvida com a sazonalidade e estações de monitoramento como fatores independentes.

A ANOVA de uma via foi aplicada para determinar a faixa de salinidade que difere significativamente ( $p < 0.05$ ) em pH no baixo do PLE. Previamente uma análise exploratória de médias e erro padrão do pH foi feita em faixas menores de salinidades de 0-5, 6-10, 11-15, 16-20, 21-25, 26-30 e >31 como foi desenvolvida por Albuquerque et al (2022). As faixas de salinidades identificadas (baixa: 0-10, mediana: 11-15 e alta > 25) e as estações foram usadas como fatores independentes em uma segunda ANOVA de duas vias

para determinar interação, efeitos e diferenças significativas sobre o pH, TA,  $p\text{CO}_2$ , pH,  $\Omega\text{Ar}$  e  $\beta\text{DIC}$ . Em ambos modelos os pressupostos de normalidade e homogeneidade da variância foram identificados. Comparações múltiplas (Teste de Tukey) foram usados para determinar as estações, sazonalidades e faixas de salinidade que diferem significativamente. Durante o período de estudo não foi feito um monitoramento constante na foz dos rios nem no oceano que permitisse a caracterização física e biogeoquímica dos *endmembers*. Entretanto, devido à região apresentar dois comportamentos dominantes (oceânico nos meses de verão-outono e fluvial nos meses de inverno-primavera; Albuquerque et al. [2002]), as seguintes restrições foram utilizadas para determinação dos *endmembers*: (i) amostras associadas às salinidades  $< 3$ , e (ii)  $> 31$  para caracterizar as situações fluvial (foz do rio) e oceânica (plataforma costeira), respectivamente. As configurações biogeoquímicas dos *endmembers* para as águas fluviais foram estimadas em  $\text{pH} = 7,55$ ,  $\text{DIC} = 617,06 \mu\text{mol kg}^{-1}$ ,  $\text{TA} = 588,52 \mu\text{mol kg}^{-1}$  e  $\beta\text{DIC} = 38 \mu\text{mol kg}^{-1}$ ; enquanto para as águas oceânicas foram estimadas em  $\text{pH} = 7,93$ ,  $\text{DIC} = 1949,22 \mu\text{mol kg}^{-1}$ ,  $\text{TA} = 2172,90 \mu\text{mol kg}^{-1}$  e  $\beta\text{DIC} = 212 \mu\text{mol kg}^{-1}$ .

### **Fator de sensibilidade e capacidade de tamponamento**

Uma forma de quantificar os impactos dos processos biogeoquímicos na alcalinidade e no pH é o uso de fatores de sensibilidade. Esses fatores representam a taxa de variação de um componente específico de um sistema devido à alteração de outro componente ( $\partial\text{response}/\partial\text{driver}$ ). Ou seja, os fatores de sensibilidade de  $\text{CO}_3^{2-}$  ( $SF\Omega$ ), pH ( $SF\beta$ ), e  $p\text{CO}_2$  ( $SFY$ ) são estimados em termos de alteração fracional por unidade de alteração de DIC. Por outro lado, a capacidade tampão expressa a capacidade de um sistema de

resistir a uma alteração de um componente que perturbe seu equilíbrio [Middelburg et al., 2020], alterando-se de forma que regule os efeitos da alteração. Essa resiliência é expressa como o inverso do fator de sensibilidade, ou seja,  $\beta_{pH}=(\partial pH/\partial DIC)^{-1}$ . Para sua análise, ambos parâmetros foram estimados usando o pacote *seacarb* do software R [Gattuso et al., 2021].

Para que fossem comparáveis com os dois sistemas estuarinos com diferente níveis de alcalinidade fluvial (alta e moderada TA fluvial) simulado por Cai et al [2021], os três fatores de sensibilidade em termos de mudança de DIC foram estimadas como as inversas de seus respetivo fatores buffer em  $(\text{mmol kg}^{-1})^{-1}$ : (a)  $SF_{CO_3^{2-}}_{DIC} = (-\omega_{DIC})^{-1}$ , (b)  $SF_{pH}_{DIC} = (\beta_{DIC})^{-1}$ , (c)  $SF_{pCO_2}_{DIC} = (Y_{DIC})^{-1}$ , e apresentados numa regressão ponderada de mínimos quadrados dos fatores acima mencionados ao longo do gradiente de salinidade. Nesta análise, a contribuição de borato ou outros componentes orgânicos dissolvidos derivados de matéria orgânica produzida localmente ou transportada de ecossistemas terrestres adjacentes não foi considerada.

### **Salinidade da Acidificação Máxima Estuarina**

Quando a água do rio com alta razão DIC/TA ( $> 1$ ) é misturada com água do mar com baixa razão DIC/TA ( $< 1$ ), ocorre um equilíbrio na concentração de íons carbonatos e dióxido de carbono em uma determinada salinidade ( $[CO_3^{2-}] \approx [CO_2]$ ), na qual a capacidade tampão da água é mínima e qualquer adição de DIC levará a uma diminuição do pH. Este ponto de equilíbrio é definido como salinidade de Máxima acidificação Estuarina (MEA). Em salinidades acima desse ponto ( $[CO_3^{2-}] > [CO_2]$ ), o sistema tem a capacidade de transformar  $CO_2$  de origem biológica ou antropogênica em  $HCO_3^-$  e a capacidade tampão aumenta com o incremento da salinidade. Por outro lado,

em salinidades mais baixas ( $[\text{CO}_3^{2-}] < [\text{CO}_2]$ ), o sistema suprime sua capacidade de tamponar as adições de  $\text{CO}_2$  [Eggleston et al., 2010; Feely et al., 2018; Cai et al., 2021]. No entanto, a capacidade tampão aumenta com o declínio da salinidade em relação à salinidade da MEA. Este aumento em baixa salinidade ( $< \text{MEA}$ ) é baseado na diluição do DIC em um *pool* de  $\text{CO}_2$  aquoso existente, no qual a mudança do pH torna-se cada vez menos sensível a novas adições de DIC conforme vai afastando-se da salinidade da MEA [Hu and Cai, 2013]. Para o cálculo foi estimada a salinidade de interceptação do  $[\text{CO}_3^{2-}]$  e  $[\text{CO}_2]$ , concentrações previamente estimadas pelo *pacote* Seacarb do software R. Esta medida ignora a contribuição de borato ou outros componentes orgânicos dissolvidos que contribuem para a alcalinidade em pH baixo.

### **Parâmetros controladores da variabilidade de pH**

A metodologia está baseada na decodificação da variação ou resposta do pH em função da variabilidade de seus quatro *drivers* ambientais (Equação 2), que são quantificados e expressos em unidades de pH, ou seja, transformando uma mudança de X em Y unidades de pH. A variabilidade de cada *driver* é obtida a partir do produto da sensibilidade ( $\partial\text{pH}/\partial\text{variável}$ ) e da variação sazonal de cada variável com base em sua média anual ( $\Delta X$ ) (Equação 3) [Takahashi et al., 2015; Middelburg et al., 2020; Cai et al., 2020].

$$\Delta\text{pH} = (\partial\text{pH}/\partial T)\Delta T + (\partial\text{pH}/\partial S)\Delta S + (\partial\text{pH}/\partial\text{DIC})\Delta\text{DIC} + (\partial\text{pH}/\partial\text{TA})\Delta\text{TA} + \dots \quad 2$$

$$\Delta X = X^{\text{Seasonal}} - X^{\text{Annual}} \quad 3$$

Na equação 1, o primeiro e o segundo termos representam os efeitos das mudanças nas constante termodinâmicas em função da temperatura (T) e salinidade (S), enquanto o terceiro e quarto termos são os fatores de

sensibilidade da mudança do pH quando o DIC e TA são alterados respectivamente [Cai et al., 2021]. Cada termo ou derivada parcial foi calculada usando a função *derivium* do pacote *seacarb* do software R (Gattuso et al., 2021). Para uma maior confiabilidade dos resultados, o fator de sensibilidade da condição considerada como oceânica na área de estudo foi calculado e comparado com os valores oceânicos reportados por Takahashi et al [2014] :  $\partial\text{pH}/\partial T = -0.014$  ( $-0.016_{\text{ocean}}$ ),  $\partial\text{pH}/\partial S = -0.0124$  ( $-0.0125_{\text{ocean}}$ ),  $\partial\text{pH}/\partial\text{DIC} = -0.0020$  ( $-0.0019_{\text{ocean}}$ ),  $\partial\text{pH}/\partial\text{TA} = +0.0020$  ( $+0.0018_{\text{ocean}}$ ).

# Capítulo V: Resultados e Discussões

Para a obtenção do título de Mestre pelo Programa de Pós Graduação em Oceanologia, é requerido que o discente realize a submissão de no mínimo um artigo científico como primeiro autor em um periódico com corpo indexado. Desse modo, os resultados da pesquisa desenvolvida no período de mestrado e a discussão dos resultados serão apresentados em forma de artigo neste capítulo. O manuscrito de autoria de Paco Quintana, Andrés Piñango, Eunice Machado e Rodrigo Kerr é intitulado *Resilience of pH to seasonal changes in a large subtropical lagoonal estuary* e encontra-se em revisão para publicação no periódico *Estuarine, Coastal and Shelf Science*.

## 1. Introduction

The acidity change of the upper ocean was around 0.1 pH unit (~30% [H<sup>+</sup>] increase) since the industrial revolution and has been unequivocally associated with the increase in greenhouse gases concentrations caused by human activities (IPCC, 2021). Its downward trend, ranging from -0.0004 to -0.0026 pH units per year between 1989 and 2014, was contrasted with a not uniform variation reported in the coastal ecosystems (-0.023 to 0.023 pH units per year), varying from acidification to basification conditions (Carstensen & Duarte, 2019). This pH variation in coastal areas has been mainly associated with metabolic processes and estuarine-ocean mixing processes at an estuary-ocean continuum in the coastal zones. Thus, both biological and physical processes acted together to influence the biogeochemical dynamics of the coastal ecosystems, leading to an increase or decline in pH depending on the water residence time (Regnier et al., 2013, Duarte et al., 2013, Cai et al., 2021). A conceptual model analyzed these sources of variability in the coastal ecosystems, defining three pH regulatory components according to Carstensen & Duarte (2019): (i) the extent of buffering of coastal waters derived from TA of the riverine endmember, (ii) the extent of mixing with ocean water, and (iii) the imbalance in ecosystem metabolism by adding or removing dissolved inorganic carbon (DIC).

Estuaries are among the most productive coastal environments, represent 0.3% of the global water surface, and are filters or exporters of nutrients and organic matter for adjacent coastal areas (Cai, 2011). The impact of anthropogenic processes due to the population increase and diversification of activities in these areas has led to an unprecedented combination of anthropogenic and

climatic stresses with effects that can alter its biogeochemical state (Paerl et al, 2006). A record of these effects was reflected in the increase of TA in the Delaware River (400-900  $\mu\text{mol kg}^{-1}$ ), Sweden River (300-460  $\mu\text{mol kg}^{-1}$ ), and the Mississippi River (1400-2800  $\mu\text{mol kg}^{-1}$ ) over the last 50-100 years, associated to weathering of carbonate rocks and the use of lime in agriculture (Duarte et al. 2013). Another record was identified in the Kemi estuary (Finland), with fluctuating interannual (1980-2017) and increasing tendency for pH (7.1-7.4) in a saline and low buffering environment, being more associated with salinity variations than with low and relatively uniform biological activity. In the Westerschelde estuary (Netherlands), the high input of organic matter in the 1970s, generated a highly heterotrophic state, with a pH of 7.63. Nevertheless, the subsequent reduction of contributions of more than 50% of the total nitrogen resulted in a pH of 7.87 in 2014, a not-so-pronounced increase due to its high buffering capacity (TA of 4000  $\mu\text{mol kg}^{-1}$ , in salinity below 2) (Hellings et al. 2013). On the other hand, the temporal or spatial extension of processes or factors forcing pH variability can induce acidic conditions, with low pH and a state of aragonite saturation ( $\Omega_{\text{Ar}}$ ). This was recorded in the Northeast Pacific coastal region of Washington state (USA) with a widespread prevalence of respiration-driven undersaturation ( $\Omega < 1$ ) in surface waters (pH  $\approx$  6.5) in fall and winter associated with the influence of net ecosystem metabolism on pH dynamics (Lowe et al., 2019).

The biogeochemical variability in the estuaries of Brazil recorded a wide TA range, between 131 and 2800  $\mu\text{mol L}^{-1}$  (1298  $\mu\text{mol L}^{-1}$ ) and a pH between 6.6 and 8.2 in the north and northeast regions. Its high negative correlation between the percentage of dissolved oxygen saturation and  $p\text{CO}_2$  suggested an intense

decomposition of organic matter in the bottom water and/or sediments resulting in pH decline in these estuarine ecosystems (Noriega & Araujo, 2014). For instance, in the eutrophic coastal waters of Guanabara Bay (RJ), the biological metabolism controlled the spatiotemporal variations of aragonite, with corrosive episodes in poorly buffered mixed waters that directly received discharges from domestic effluents and polluted rivers. In contrast, the high values were recorded in upper-middle stratified surface water, dominated by phytoplankton blooms and high buffer capacity (Cotovicz et al., 2017). A different scenario was observed in the oligotrophic São Francisco estuary, whose warm and poorly buffered waters with a short residence time promoted the predominance of the thermodynamic equilibrium of carbonate over biological processes, determining the water-air CO<sub>2</sub> fluxes in mixing periods (Abril et al., 2021). In the warm hypersaline Araruama coastal lagoon dominated by phytoplankton blooms, high pH and buffer capacity added to the net autotrophic metabolisms and pCO<sub>2</sub> increase driven by CaCO<sub>3</sub> precipitation, generated a net annual CO<sub>2</sub> sink. Part of the higher values of pCO<sub>2</sub> in summer in contrast to winter were associated with the thermodynamic effects caused by the warming water and the increase of salinity (Cotovicz et al., 2021).

In the lower estuarine zone of PLE, Albuquerque et al. (2022) used a monthly evaluation from 2017 to 2021 and reported an alkaline environment in surface waters characterized by an average pH of 8.0 and CaCO<sub>3</sub> supersaturation conditions. A significant seasonal variation in the water-air CO<sub>2</sub> fluxes was identified in the region, which was associated with the seasonal pattern of freshwater discharge. Although the PLE behaved as a net CO<sub>2</sub> sink zone between 2017-2021, the region has been also experiencing periods of both

CO<sub>2</sub> ingassing (December and May) and outgassing (June and November), which is mainly marked at the inner zones of the region (Albuquerque et al., 2023). In addition, a daily evaluation study of the pelagic ecosystem metabolism in the PLE channel determined predominantly heterotrophic conditions and evidence of the Plata River plume intrusion in the summer of 2021, likely altering and regulating the local biogeochemistry in the period analyzed (Bordin et al., 2023).

Although the aforementioned studies have reported the first evaluation of how the CO<sub>2</sub>-carbonate chemistry evolved in the PLE, they do not infer about the buffering capacity or determine the effect of acidification on biocalcification (e.g., Li et al., 2020). Those studies were based on the temporal analysis of pH, TA, or  $\Omega_{Ar}$ , however, these parameters did not quantify the resilience (i.e., the resistance to change) of the system under the pressure of a driver along a salinity gradient. In some studies, the Revelle factor was commonly used to quantify the response of the CO<sub>2</sub>-carbonate system to CO<sub>2</sub> additions, however, it does not explain the pH response (Hu & Cai, 2013; Middelburg et al., 2020; Cai et al., 2020). Thus, the current study used the  $\beta$ DIC factor proposed by Egleston et al. (2020) as a direct measure of the pH response to DIC additions, to determine and quantify the buffering of pH at two stations in the lower zone of the PLE. In addition, we estimated the effects of environmental drivers on pH to infer the processes (or forcing factors) responsible for its seasonal variability. This research significantly contributes to the observational and methodological knowledge of the pH research in estuarine systems at a regional scale in the southern hemisphere, specifically in southern Brazil. In addition, the results presented here allowed further questions to better understand the effects of pH

changes in the study region, such as determining the saturation threshold of the organisms in that ecosystem or a spatial analysis to determine the area that presents the best buffer conditions against seasonal pH changes to reduce or mitigate the effects of this variability on resources, essential for aquaculture development.

### **1.2. Patos Lagoon Estuary Features**

Patos Lagoon is the largest coastal lagoon in Brazil, located between 30°S and 32°S in the state of Rio Grande do Sul (RS), covering an area of 10,360 km<sup>2</sup> and a drainage basin of approximately 200,000 km<sup>2</sup> connected to the South Atlantic Ocean through a canal in the city of Rio Grande (Seeliger, 2001; Lemke et al., 2007). This ecosystem is classified as a shallow coastal lagoon, with an average depth of 5-6 m. It presents a NE-SW orientation, parallel to the RS coastline and to the prevailing wind direction, which is the main forcing of its hydrodynamic regime, with an astronomical tidal amplitude of 0.45 m (Marinho et al., 2020). Its distribution encompasses subtropical and warm temperate regions with a mean air temperature of 18 °C, a maximum annual precipitation that oscillates between 1200 and 1500 mm (Abreu et al., 2016), and an average annual river discharge of about 2400 m<sup>3</sup>s<sup>-1</sup> (Andrade et al., 2022).

The late winter period and the spring season register the greatest freshwater discharge, contrary to autumn where the greatest intrusion of seawater and the least contribution of freshwater occur, resulting in the flooding and salinization of the Patos Lagoon Estuary (PLE) (Möller et al., 2001). This intrusion of saline water is limited to the lower estuary, which represents 10% of the total area of the lagoon, causing a wide salinity gradient from 0-35 (Seeliger, 2001; Vaz et al., 2006). At the trophic level, the central channel of the lower estuary presents

a predominantly balanced condition, classified as mesotrophic, due to its high capacity for self-purification through dilution, which is facilitated by the greater hydrodynamics and shorter residence time of the water masses in the channel (Baumgarten et al., 2013). At the biogeochemical level, the dominant mechanisms responsible for the variability of the parameters of the carbonate system are the dilution and concentration of salts. These processes defined by their hydrological patterns suggest two scenarios of the estuarine biogeochemical conditions: (I) ocean-dominated during summer and autumn, and (II) river-dominated during winter and spring, this last scenario with a greater susceptibility to undersaturation conditions (Albuquerque et al., 2022).

Despite the short residence time of approximately two days (Gordey & Osadchiv, 2022), the lower estuary presents a disparity between its zones, as occurs in the mouth of the estuary (hereafter referred to as outer zone), which is predisposed to strong currents with residence time slightly shorter than the shallow and embayment zones (hereafter referred to inner zone), which present a partially restricted circulation (Albuquerque et al., 2022). This is expressed in the considerable differences exhibited in the concentration and variability of phytoplankton, probably associated with the different hydrological conditions (Abreu et al., 2016). The two zones host two continuous monitoring stations (Fig. 1) of the Brazilian Ocean Acidification Network program (BrOA Network; [www.broa.furg.br/](http://www.broa.furg.br/); Kerr et al., 2016) and of the Brazilian Long Term Ecological Research (BR-LTER) of PLE and Adjacent Marine Coast program ([www.peld.furg.br](http://www.peld.furg.br/); Odebrecht and Abreu, 2019). The first station (BrOA-1) is in an inner inlet. Its shallow depth (< 2 m) and low hydrodynamic regime make the wind its main forcing that stimulates the mixing of the water column and

exchange with the bottom sediments. In addition, this station is predisposed to the influence of industrial and domestic sewage from Rio Grande City. The second station (BrOA-2) is located near the mouth of the estuary. Its higher depth and greater influence of intrusions from the South Atlantic Ocean and the influence of the wind favor the formation of vertical salinity structures that oscillate from a salt wedge to a well-mixed gradient (Möller et al., 2001).

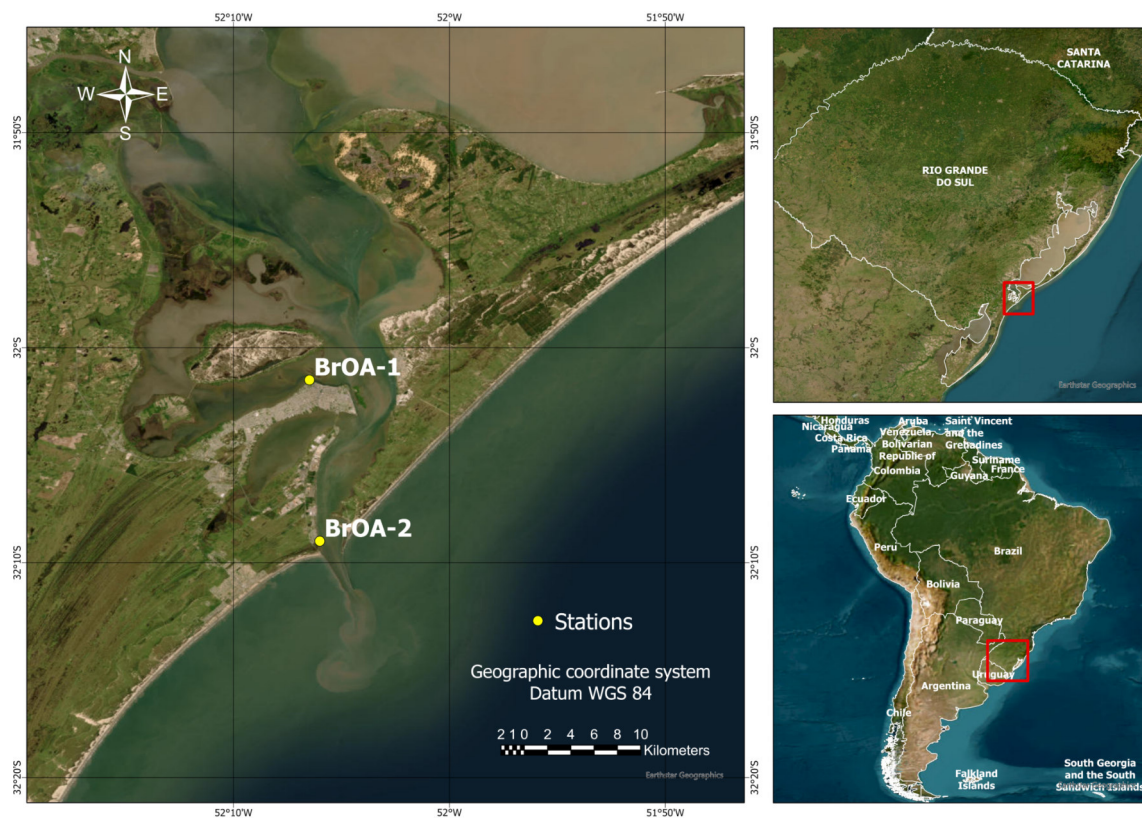


Figure 1. Map of the lower estuarine zone of the Patos Lagoon Estuary (left) with the location of pier-fixed monitoring stations BrOA-1 and BrOA-2 (yellow dots). The right maps show the location of the estuarine zone of the Patos Lagoon (upper) and the Rio Grande do Sul State (bottom), both marked as red rectangles.

## 2. Material and Methods

### 2.1. Sampling strategy

The database is part of two large monitoring programs, BrOA Network (started in October 2015) and LTER-PLE, the latter with the largest temporal dataset

(since 1998) on estuarine and marine biota and abiotic parameters in the Southern Hemisphere (Lemos et al., 2022). The data, in a monthly frequency for the period May 2017 - November 2022, includes the parameters temperature, salinity, concentrations of dissolved inorganic nutrients and chlorophyll (Chl-a) from the LTER program, and total alkalinity and pH of the BrOA Network program. In both monitoring, the parameters were obtained and measured from water samples collected with a 5 L van Dorn bottle at 1 m below the surface at pier-fixed stations located in the inner and outer zones (Fig.1) in the lower estuary.

## ***2.2. Temperature, salinity, nutrients, and chlorophyll a***

The temperature was measured in situ using a digital thermometer while the salinity was measured in the laboratory with a Metrohm® 914 conductivity meter. The inorganic nutrients and Chl-a were collected in plastic bottles and preserved in cold storage for later analysis in the laboratory. For the analysis of inorganic nutrients (silicic acid, phosphate, nitrite, and nitrate), the samples were filtered through cellulose acetate membrane filters and measured using a SEAL Analytical Autoanalyzer AA3 HR according to the methodology described by Grasshoff et al. (2009). In the case of the concentration of Chl-a, an aliquot of 50-250 mL was filtered (depending on the material concentrated) through Whatman GF/F filters under dim light and forthwith frozen ( $-80^{\circ}\text{C}$ ) for afterward be measured using a calibrated Turner Designs TD-700 fluorometer with correction for degradation product, using the non-acidification method described by Welshmeyer (1994).

### **2.3. Total alkalinity and pH**

The TA samples were collected in 500 mL borosilicate glass bottles following the procedure described by Dickson et al. (2007). To prevent any biological activity, the samples were immediately fixed with mercury chloride solution and subsequently refrigerated to prevent evaporation. Laboratory analysis was performed through closed cell potentiometric titration (Dickson et al, 2007) using an automated titrator (Metrohm® Titrand 888) and a combined glass reference electrode (Metrohm® 6.0262.100) at a controlled temperature from  $25 \pm 0.1^\circ\text{C}$  supported by thermostatic bath. Due to the wide range of salinity present in the estuary, an adaptation of the closed cell method was adopted and described by Albuquerque et al. (2022). The daily evaluation with replicates of a single sample allowed us to evaluate the consistency of the measurements whose analysis precision was  $4 \mu\text{mol kg}^{-1}$  with a range between 2.3 and  $5 \mu\text{mol kg}^{-1}$ .

The pH samples were collected in 125 mL amber borosilicate flasks and preserved under shade in a styrofoam, keeping its temperature. Each sample was measured (within 2 hours of sampling) using a Metrohm® 913 or 914 pH meter coupled to a glass-reference electrode cell and temperature sensor. These instruments were previously standardized using Fluka buffer solutions of pH 4.00 and 7.41 at  $25^\circ\text{C}$  until January 2021, and subsequently with Merck Certipur buffer solutions of pH 4, 7, and 9 at  $20^\circ\text{C}$ . In order to obtain better precision and accuracy, two replicates were collected and read for each point of the same water sample collected; in addition to ejecting regular measurements of the buffer solution at  $\text{pH} = 7$  during the analysis. The measurement uncertainty was  $< 0.05$  NBS unit and the values were corrected to in situ

temperature by the equation developed by Gieskes (1969). The total scale was chosen and further used for pH at in situ temperature.

#### **2.4. Data processing and statistical analysis**

The parameters of the carbonate system and pH scale conversion were estimated with the macro tool CO<sub>2</sub>sys\_v3.0\_err.xlsm version 3.0, developed by Lewis et al. (1998) and modified by Pierrot et al. (2021), using as input parameters, temperature, salinity, TA, pH, and silicic acid and phosphate concentrations. Due to the wide variation in salinity and temperature, the  $k_1$  and  $k_2$  dissociation constants reported by Millero (2010) were chosen, as in the research of Hu et al. (2017), McCutcheon et al. (2019) and McCutcheon and Hu (2022) to estuarine system. In addition, the sulfate and borate constants reported by Dickson (1990) and Lee et al. (2010), respectively, were used. The propagated error defined as an estimate of the error associated with the selection of variables and constants for calculating the parameters of the carbonate system was determined by the method reported by Orr et al. (2018) using the seacarb package (Gattuso et al., 2021). Each estimated variable presented a mean uncertainty with a standard error of DIC:  $14 \pm 0.7 \mu\text{mol kg}^{-1}$ ,  $p\text{CO}_2$ :  $75 \pm 3 \mu\text{atm}$ ,  $\Omega\text{Ar}$ :  $0.10 \pm 0.007$ ,  $\Omega\text{Ca}$ :  $0.17 \pm 0.012$ ,  $\text{CO}_2$ :  $2.9 \pm 0.12 \mu\text{mol kg}^{-1}$  and  $\text{CO}_3^{2-}$ :  $6.7 \pm 0.50 \mu\text{mol kg}^{-1}$  (Table S.1). In the pH scale conversion, the pH at total scale ( $\text{pH}_{\text{Total}}$ ) registered a mean difference of 0.142 units lower than the NBS scale, a value not far from what is described in the macro that estimates a residue of 0.13 at a salinity of 20, a temperature of 25°C and a pressure of 1 atm.

Descriptive statistics, normality tests, and Box-Cox transformation were performed to identify outliers and meet parametric assumptions using R

software (version 4.2.2, 2022). To assess temporal and/or spatial variability of the buffering capacity, a two-way analysis variance (ANOVA) was employed on the parameters of the carbonate system. Seasonality and stations (BrOA-1<sub>inner</sub> and BrOA-2<sub>outer</sub>) were treated as independent factors in the analysis.

On the other hand, to ascertain the significant differences ( $p < 0.05$ ) in pH within the lower PLE across distinct salinity ranges, a one-way ANOVA was conducted on pH. The salinity ranges (0–5, 6–10, 11–15, 16–20, 21–25, 26–30, and >31) analyzed by Albuquerque et al. (2022) were employed as independent factors. Subsequently, ranges displaying similarity were consolidated into low (0-10), medium (11-25), and high (>25) salinity categories. These categories were then utilized alongside the stations as independent factors in a two-way ANOVA to evaluate interactions, effects, and significant differences on pH, TA,  $p\text{CO}_2$ ,  $\Omega\text{Ar}$ , and  $\beta\text{DIC}$ . In both models, the assumptions of normality and homogeneity of variances were confirmed. Finally, a multiple comparison test (Tukey's Honest Significant Difference) was used to assess the stations, seasons, or salinity ranges that exhibited significant differences.

During the study period, there was no constant monitoring at the mouth of the river nor in the ocean that would allow the physical and biogeochemical characterization of the endmembers. However, due to the region presenting two dominant behaviors (oceanic in the summer-autumn months and fluvial in the winter-spring months; Albuquerque et al. (2022), the following restrictions were used to determine the endmembers: (i) associated samples to salinities  $< 3$ , and (ii)  $> 31$  to characterize the fluvial (river mouth) and oceanic (coastal platform) conditions, respectively. The biogeochemical settings of the riverine endmember were estimated at  $\text{pH} = 7.58$ ,  $\text{DIC} = 617.06 \mu\text{mol kg}^{-1}$ ,  $\text{TA} = 588.52$

$\mu\text{mol kg}^{-1}$  and  $\beta\text{DIC} = 38 \mu\text{mol kg}^{-1}$ , while for the ocean endmember they were  $\text{pH} = 7.93$ ,  $\text{DIC} = 1949.22 \mu\text{mol kg}^{-1}$ ,  $\text{TA} = 2172.90 \mu\text{mol kg}^{-1}$  and  $\beta\text{DIC} = 212 \mu\text{mol kg}^{-1}$ .

## **2.5. Sensitivity factor and buffer capacity**

One way to quantify the impacts of biogeochemical processes on alkalinity and pH are sensitivity factors. These represent the rate of change of a specific component of the system by the alteration of another ( $\partial\text{response}/\partial\text{driver}$ ), i.e., the sensitivity factor of  $\text{CO}_3^{2-}$  ( $\partial\text{CO}_3^{2-}/\partial\text{DIC}$ ), pH ( $\partial\text{pH}/\partial\text{DIC}$ ),  $\text{pCO}_2$  ( $\partial\text{pCO}_2/\partial\text{DIC}$ ) in terms of fractional change per unit change of DIC. On the other hand, the buffer capacity expresses the ability of the system to resist the alteration of a component that disturbs its balance (Middelburg et al., 2020), changing in such a way that the effects of the alteration are regulated. This buffering is expressed as the inverse of the sensitivity factor, i.e.  $\beta_{\text{pH}} = (\partial\text{pH}/\partial\text{DIC})^{-1}$ , and was estimated using the seacarb package of R software (Gattuso et al., 2021).

In order to ensure comparability with the two distinct estuarine systems characterized by varying river alkalinity levels (high and mid-TA river) as simulated by Cai et al. (2021), the three sensitivity factors concerning changes in DIC were calculated as the reciprocals of their respective buffer factor in ( $\text{mmol kg}^{-1}$ )<sup>-1</sup>: (a)  $\partial\text{CO}_3^{2-}/\partial\text{DIC} = (-\omega_{\text{DIC}})^{-1}$ , (b)  $\partial\text{pH}/\partial\text{DIC} = (\beta_{\text{DIC}})^{-1}$ , (c)  $\partial\text{pCO}_2/\partial\text{DIC} = (Y_{\text{DIC}})^{-1}$ . The data for each factor were displayed in a scatter plot along with its corresponding weighted least squares regression fit and confidence bands for each station across the salinity gradient (Fig.S.1). In this analysis, the potential contribution of borate or other dissolved organic

components derived from locally produced organic matter or transported from adjacent terrestrial ecosystems was not considered.

## **2.6. Maximum Estuarine Acidification Salinity**

When river water with a high DIC/TA ratio ( $> 1$ ) mixes with seawater with a low DIC/TA ratio ( $< 1$ ), an equilibrium is established in the concentrations of carbonate ion and carbon dioxide at a specific salinity ( $[\text{CO}_3^{2-}] \approx [\text{CO}_2]$ ). At this salinity the water buffering capacity is minimum and any addition of DIC will result in a maximum reduction in pH. This point of equilibrium is termed as Maximum Estuarine Acidification (MEA) salinity. On the higher-salinity side of this point (i.e.,  $[\text{CO}_3^{2-}] > [\text{CO}_2]$ ), the system can convert anthropogenic or biologically produced  $\text{CO}_2$  to  $\text{HCO}_3^-$ , and the buffering capacity increases as salinity increases. In contrast, on the lower-salinity side (i.e.,  $[\text{CO}_3^{2-}] < [\text{CO}_2]$ ), the system has essentially lost its capacity to buffer  $\text{CO}_2$  additions (Egleston et al., 2010; Feely et al., 2018; Cai et al., 2021). Nevertheless, the buffering capacity rises as salinity decreases, particularly in relation to the MEA salinity. This heightened capacity at lower salinities ( $<$  MEA salinity) arises due to the dilution of DIC into the existing aqueous  $\text{CO}_2$  pool. Consequently, the pH alteration becomes less responsive to additional DIC inputs compared to the MEA salinity scenario (Hu and Cai, 2013). The MEA salinity was determined through the intersection of  $[\text{CO}_3^{2-}]$  and  $[\text{CO}_2]$  in relationship to salinity. Previously, the ions were calculated using the package Seacard of R software. This measure ignores the contribution of borate or other dissolved organic components that contribute to alkalinity at low pH.

## 2.7. Drivers of pH variability

This method is based on decoding the variation or response of pH as a function of the variability of its four environmental drivers (Equation 1), which are quantified and expressed in pH units, i.e., transform a change in X into Y pH units. The variability of each driver is obtained from the product of the sensitivity factor ( $\partial\text{pH}/\partial\text{parameter}$ ) and the seasonal change of each parameter based on its annual mean ( $\Delta X$ ) (Equation 2) (Takahashi et al., 2014; Middelburg et al., 2020; Cai et al., 2021).

$$\Delta\text{pH} = (\partial\text{pH}/\partial T)\Delta T + (\partial\text{pH}/\partial S)\Delta S + (\partial\text{pH}/\partial\text{DIC})\Delta\text{DIC} + (\partial\text{pH}/\partial\text{TA})\Delta\text{TA} + \dots 1$$

$$\Delta X = X^{\text{Seasonal}} - X^{\text{Annual}} \quad 2$$

In the equation 1, the first ( $\partial\text{pH}/\partial T$ ) and second ( $\partial\text{pH}/\partial S$ ) terms represent the effects of changes in thermodynamic constants with respect to temperature (T) and salinity (S), while the third ( $\partial\text{pH}/\partial\text{DIC}$ ) and fourth ( $\partial\text{pH}/\partial\text{TA}$ ) are the sensitivity factors of pH change in response to variation in DIC and TA, respectively (Cai et al., 2021). Each term or partial derivative was computed using the function *derivnum* of the *seacarb* package of R software to both BrOA-1 and BrOA-2 (Gattuso et al., 2021). To enhance the reliability of the outcomes, the sensitivity factors of the ocean endmember were calculated and compared with the oceanic values reported by Takahashi et al. (2014):  $\partial\text{pH}/\partial T = -0.014$  ( $-0.016_{\text{ocean}}$ ),  $\partial\text{pH}/\partial S = -0.0124$  ( $-0.0125_{\text{ocean}}$ ),  $\partial\text{pH}/\partial\text{DIC} = -0.0020$  ( $-0.0019_{\text{ocean}}$ ),  $\partial\text{pH}/\partial\text{TA} = +0.0020$  ( $+0.0018_{\text{ocean}}$ ).

### 3. Results

#### 3.1. Statistical analysis

A two-way ANOVA was performed to analyze the temporal and spatial effect on the variables that determine and quantify the buffering capacity in the estuarine region of the Patos Lagoon. The model revealed that there was not significant interaction between the seasonality and the stations on salinity, pH, TA,  $\Omega\text{Ar}$ ,  $p\text{CO}_2$ , and  $\beta\text{DIC}$ . The locations of stations (BrOA-1<sub>inner</sub> and BrOA-2<sub>outer</sub>) had a significant effect on pH [ $F_{(3,170)} = 4.73$ ,  $p < 0.05$ ] and  $p\text{CO}_2$  [ $F_{(3,170)} = 7.05$ ,  $p < 0.01$ ] meanwhile the seasonality had a statistically significant effect on all parameters of carbonate systems (Table S.2).

A post hoc Tukey test showed that salinity, pH, TA, and  $\Omega\text{Ar}$  (Fig 2.a-d) differed significantly ( $p < 0.05$ ) between summer with both winter and spring in BrOA-1. In the same station, the  $p\text{CO}_2$  (Fig 2.e) recorded a dissimilarity between summer and spring, while the buffering of pH to change of DIC (Fig 2.f) only differed between summer and winter. By contrast, the salinity, pH, TA, (Fig 2.a-c)  $p\text{CO}_2$ , and  $\beta\text{DIC}$  (Fig 2.e-f) did not reveal seasonal differences in the BrOA-2 station. The  $\Omega\text{Ar}$  (Fig 2.d) was the only parameter that reported a temporal difference between summer and winter.

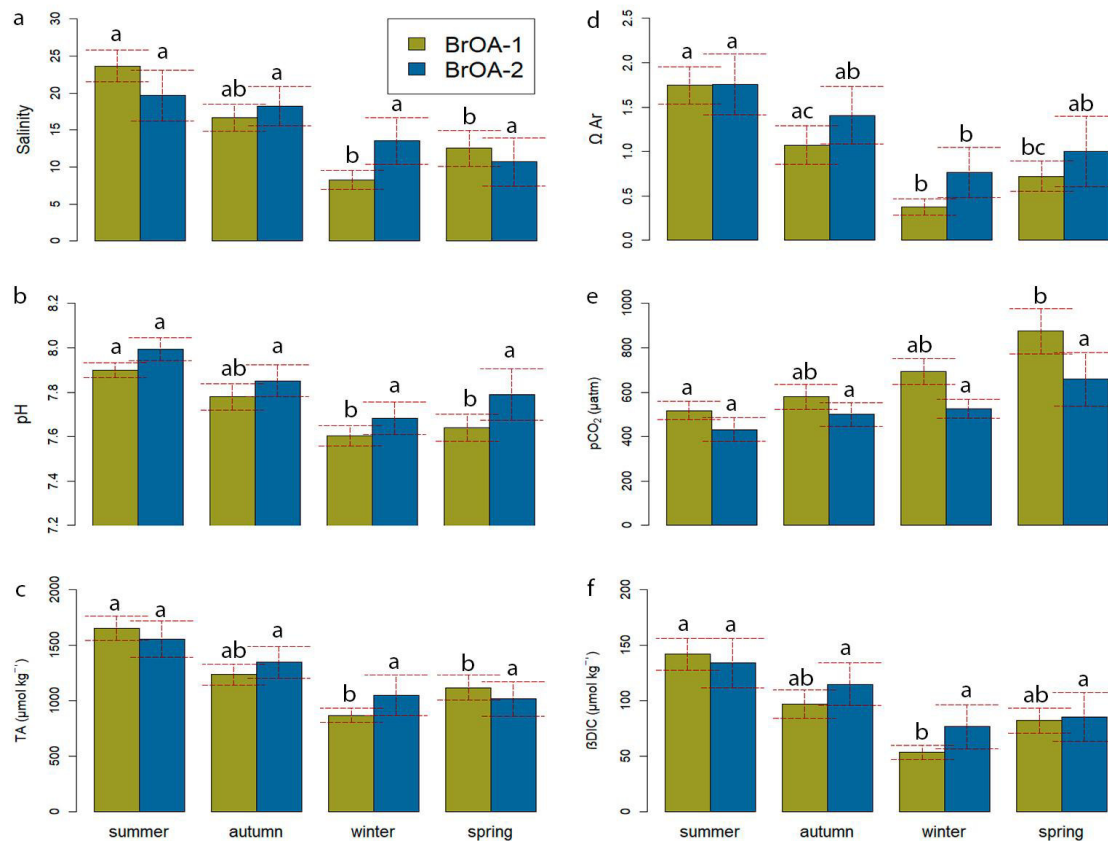


Figure 2. Means ( $\pm$  standard error) and two-way ANOVA results for six parameters of the carbonate system: (a) salinity, (b) pH at total scale, (c) total alkalinity (TA), (d) state aragonite saturation ( $\Omega_{Ar}$ ), (e) partial pressure of carbon dioxide ( $pCO_2$ ), (f) buffer capacity of pH to fractional change of dissolved inorganic carbon ( $\beta DIC$ ), recorded seasonally for 2 monitoring stations (BrOA-1 and BrOA-2) in the lower zone of Patos Lagoon Estuary. Different letters indicate significant differences between the seasonality within stations, at  $p < 0.05$  with Tukey's tests following post-ANOVA. Note, for instance, the salinity in (a) did not show seasonal differences in the BrOA-2, in opposition to BrOA-1 where the summer differed significantly from both winter and spring.

In the second two-way ANOVA was analyzed the effect of each salinity range on the carbonate system parameters in the two monitoring stations (Table S.3). The model revealed a salinity effect on all parameters, contrary to the spatial effect that was only significant on pH [ $F_{(1,172)} = 5.69$ ,  $p < 0.05$ ] and  $pCO_2$  [ $F_{(1,172)} = 6.94$ ,  $p < 0.01$ ] with spatial significant differences ( $p < 0.05$ ). Both independent factors only had statistically significant interaction on  $\beta DIC$  [ $F_{(2,170)} = 3.58$ ,  $p < 0.05$ ] (Table S.3).

In the post hoc Tukey test, the pH differed significantly in low with both medium and high salinity in the BrOA-1 station, in contrast to BrOA-2, whose dissimilarity was reported between low and high salinity (Fig 3.a). The TA (Fig 3.b),  $\Omega$ Ar (fig 3.c) and  $\beta$ DIC (fig 3.e) differed significantly ( $p < 0.05$ ) in all ranges of salinity with spatial differences reported in the buffer factor in low salinity. The  $p\text{CO}_2$  (fig 3.d) was the only parameter that reported similarity in each range of salinity in both stations.

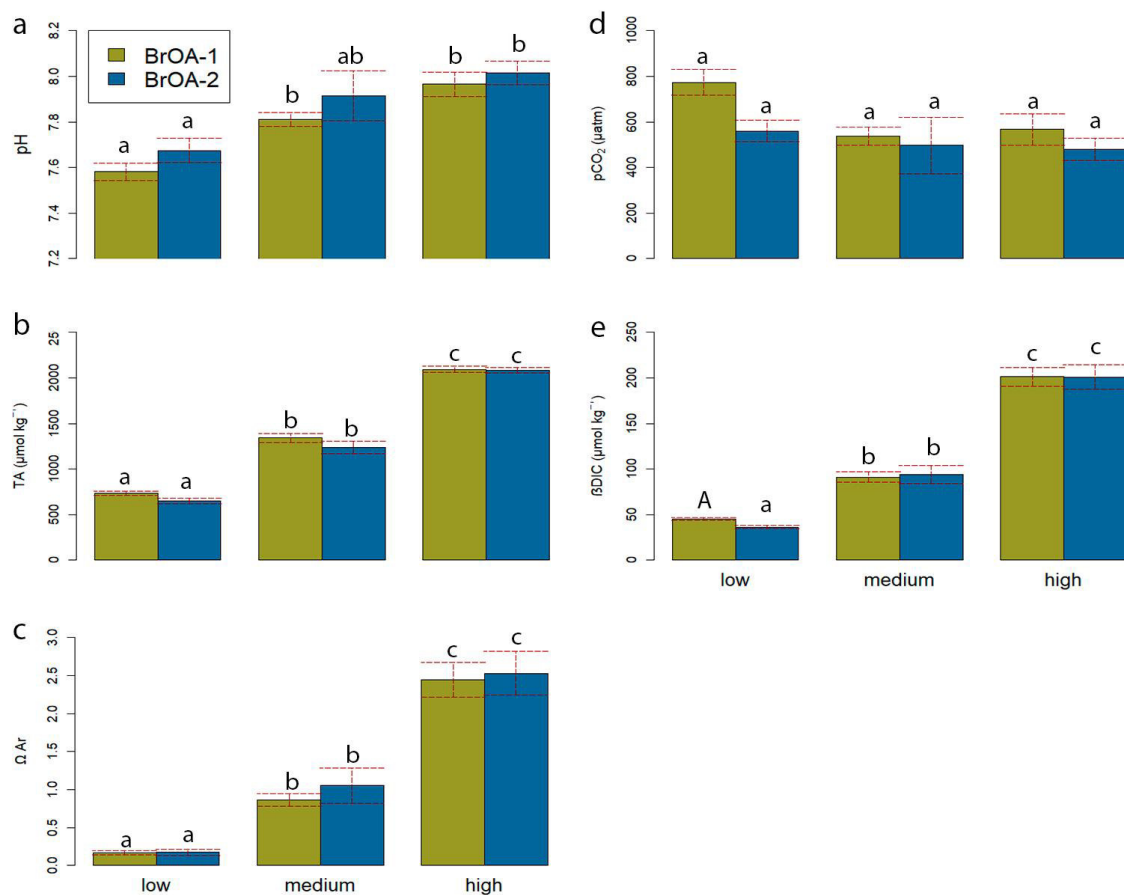


Figure 3. Means ( $\pm$  standard error) and two-way ANOVA results for 5 parameters of the carbonate system: (a) total alkalinity (TA), (b) pH at total scale, (c) state aragonite saturation ( $\Omega$ Ar), (d) partial pressure of carbon dioxide ( $p\text{CO}_2$ ), (e) buffer capacity of pH to fractional change of dissolved inorganic carbon ( $\beta$ DIC), recorded for each range of salinity (low: 0-10, medium: 11-25, high >25) in the 2 monitoring stations (BrOA-1 and BrOA-2) in the lower zone of Patos Lagoon Estuary. Different letters indicate significant differences between the salinity ranges within stations at  $p < 0.05$  with Tukey's tests following post-ANOVA. Capital letters show significant differences between stations in the same salinity range. Note, for instance, the pH (a) showed differences between low and high salinities in BrOA-2, in opposition to BrOA-1 where the low differed significantly from medium and high salinities.

### **3.2. Sensitivity factor and buffer capacity**

The rate of change or sensitivity factor of  $p\text{CO}_2$ , pH, and  $\text{CO}_3^{2-}$  per DIC unit were higher in low-salinity estuarine waters than in seawater (Fig. S.1). Throughout the salinity gradient, the sensitivity of  $p\text{CO}_2$  was greater than pH and  $\text{CO}_3^{2-}$ , this last one presenting the lowest sensitivity. The salinity effect on pH sensitivity to DIC alteration was significant [ $F_{(2,172)} = 366.2$ ,  $p < 0.001$ ] along the salinity gradient with an interaction with the station effect [ $F_{(2,172)} = 3.58$ ,  $p < 0.05$ ] and spatial differences in low salinity ( $p < 0.05$ ).

Complementary, the  $\beta\text{DIC}$  was analyzed with Aragonite saturation along the salinity gradient to estimate the range that characterized low buffering in the lower estuary, considering that  $\Omega=1$  is the reference abiotic threshold for  $\text{CaCO}_3$  dissolution and calcification (Feely et al. 2018). In this relationship, the subsaturation points presented a distribution associated mainly with the buffering capacity that defined the riverine endmember ( $\beta\text{DIC}=38 \mu\text{mol kg}^{-1}$ ), however, some points were identified near  $\beta\text{DIC}$  means of both stations. In relation to salinity, its dispersion was observed in almost the entire gradient, with records even in high salinity in BrOA-1 station, and in medium salinities in BrOA-2 (Fig.4).

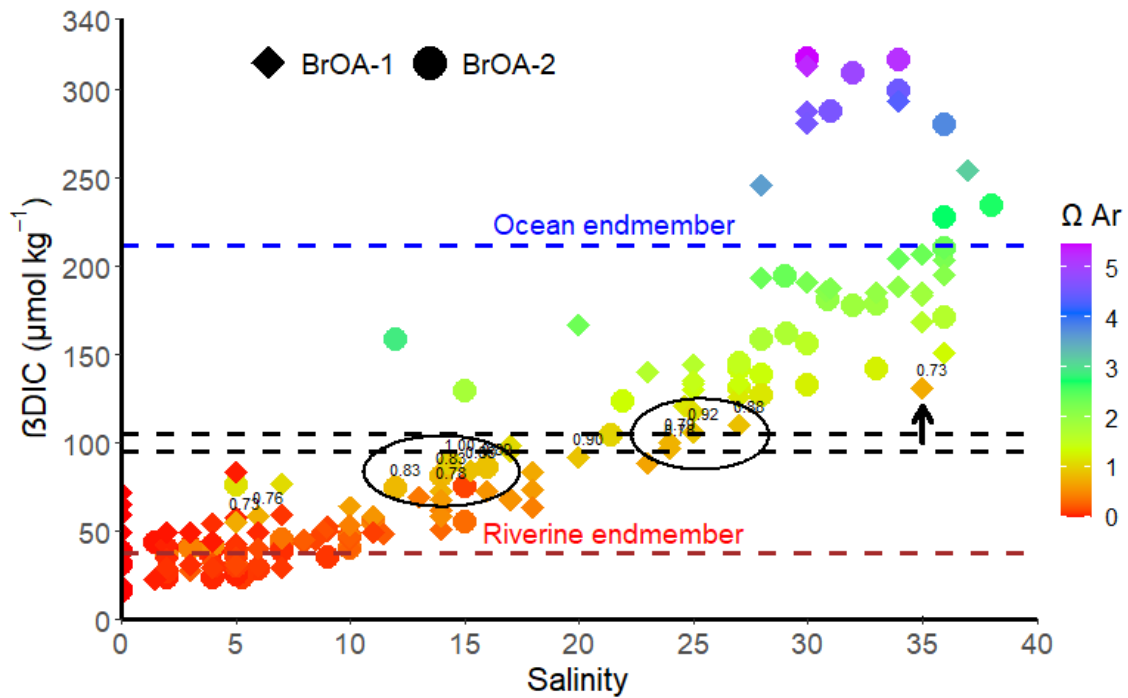


Figure 4. Distribution of the buffer capacity of pH to fractional change of DIC ( $\beta\text{DIC}$ ) in relation to salinity and  $\Omega\text{Ar}$  (color bar) in the BrOA-1 (diamond) and BrOA-2 (circle) stations in the lower zone of Patos Lagoon Estuary. The dotted lines correspond to the  $\beta\text{DIC}$  estimated to riverine endmember ( $\beta\text{DIC}_{\text{river}} = 38 \mu\text{mol kg}^{-1}$ ; red dashed line), station means ( $\beta\text{DIC}_{\text{BrOA-1}} = 95 \mu\text{mol kg}^{-1}$  and  $\beta\text{DIC}_{\text{BrOA-2}} = 105 \mu\text{mol kg}^{-1}$ ; black dashed lines) and ocean endmember ( $\beta\text{DIC}_{\text{ocean}} = 212 \mu\text{mol kg}^{-1}$ ; blue dashed line). The arrows and ellipses indicate the values closest to the saturation threshold for each station.

A temporal variability analysis of pH recorded values below their annual mean between August to October ( $>7.83$ ) and July to October ( $>7.73$ ) to the BrOA-2 and BrOA-1 stations respectively (Fig. 5.A-B). In contrast, December to March had the highest records above the mean in the BrOA-2 station, while this pattern was limited to the period from January to April at the BrOA-1 station. The pH buffering exhibited a similar variability to salinity, with consistently high values above its mean ( $105 \mu\text{mol kg}^{-1}$ ) in the first semester, followed by a significant decline from August to November in the BrOA-2 station (Fig 5.C). The BrOA-1 displayed a continuous decrease of salinity and  $\beta\text{DIC}$  from March to October, with a sharp increase in the last months (Fig 5.D). On the other hand, chl-a concentrations reached their peak in the months of January,

October, and November; recording in November the lowest record of salinity and buffering capacity in the BrOA-2 station. In the case of BrOA-1, the chl-a remained constant in the first semester, with its highest values observed in July, October, and November.

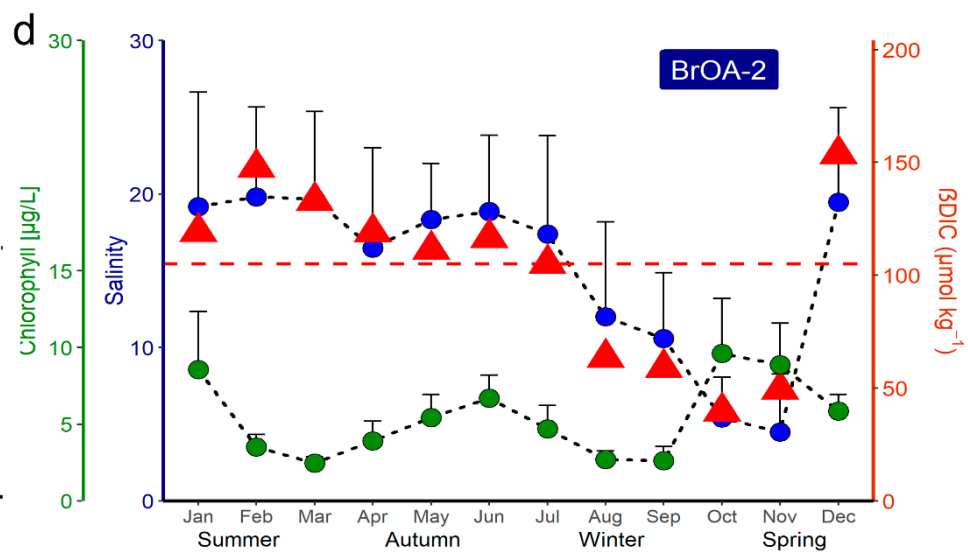
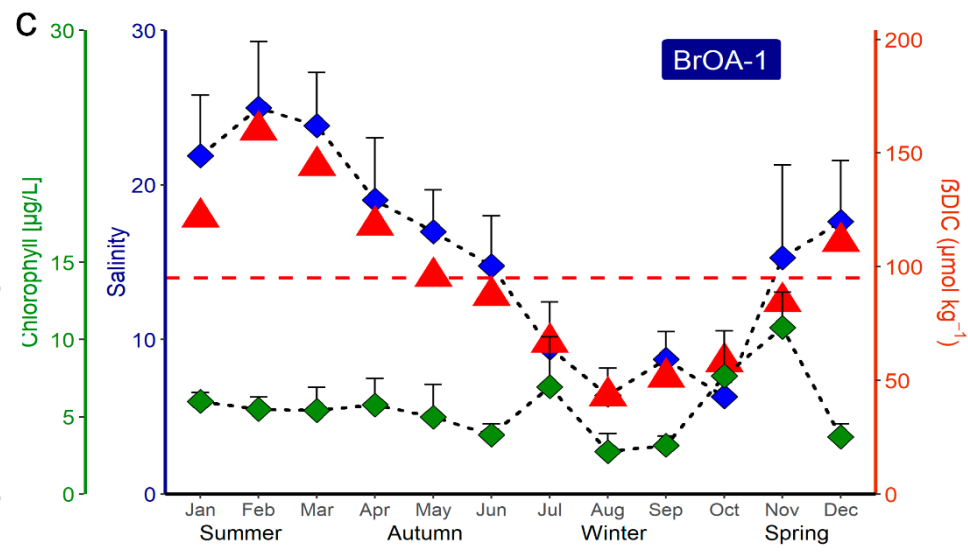
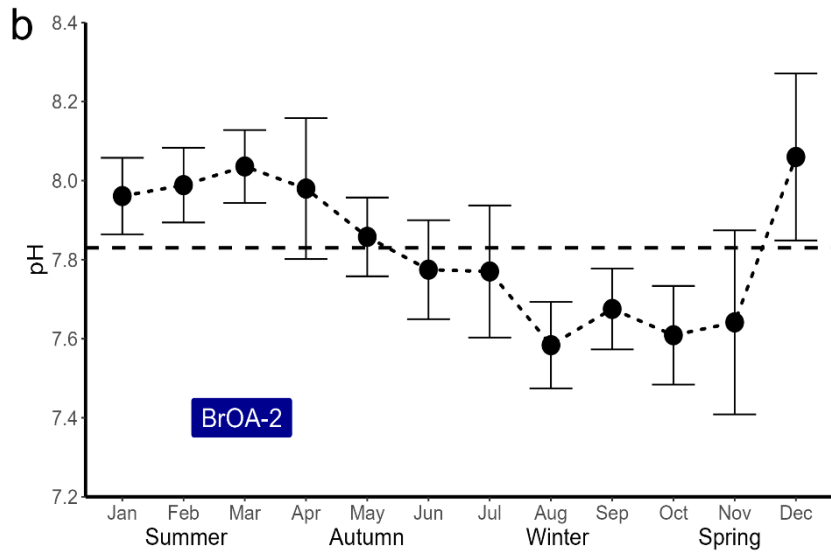
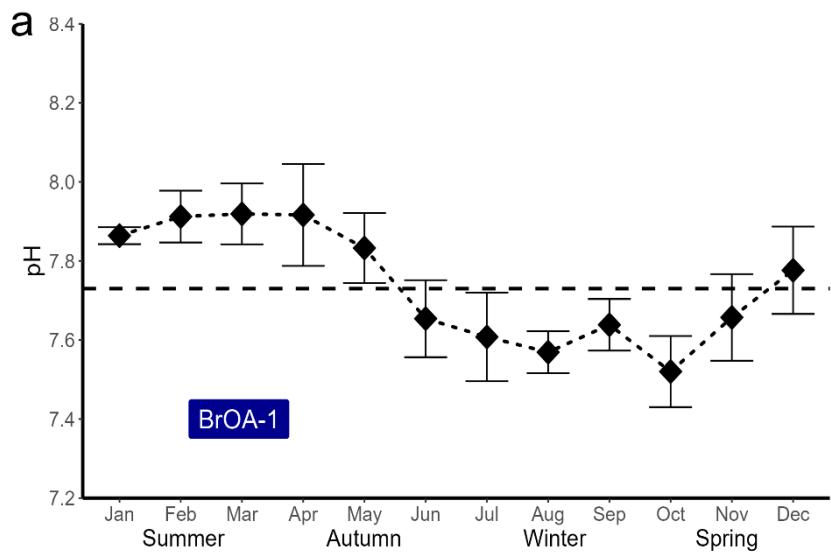


Figure 5. Monthly variability of pH at total scale in the BrOA-1 (A) and BrOA-2 (B) stations of the lower zone of Patos Lagoon Estuary. Monthly variability of the salinity and chlorophyll-a associated with the buffer capacity of pH to fractional change of dissolved inorganic carbon ( $\beta$ DIC) in the BrOA-1 (C) and BrOA-2 (D) stations. The dotted lines correspond to the mean estimated to pH ( $\text{pH}_{\text{BrOA-1}} = 7.7$  and  $\text{pH}_{\text{BrOA-2}} = 7.83$ ; black dashed line), and  $\beta$ DIC to both stations ( $\beta\text{DIC}_{\text{BrOA-1}} = 95 \mu\text{mol kg}^{-1}$  and  $\beta\text{DIC}_{\text{BrOA-2}} = 105 \mu\text{mol kg}^{-1}$ ; red dashed lines).

### 3.3. Maximum Estuarine Acidification Salinity

The salinities more susceptible, where any DIC addition alters the pH of the system, were recorded in 9.5 and 6.5 at BrOA-1 and BrOA-2, respectively. For the BrOA-1 station, only the summer registered a MEA salinity lower than its mean, while the other seasons presented an equanimous distribution near its mean, with the highest record in spring (11). In BrOA-2 was observed a seasonal equanimity between warm and cold seasons based on its mean, with seasonal limits in summer ( $< 1$ ) and winter ( $\approx 10$ ) (Table 1).

Table 1. Maximum estuarine acidification (MEA) salinity estimates derived from the intersection of CO<sub>2</sub> and CO<sub>3</sub><sup>2-</sup> concentrations as a function of the salinity for BrOA-1 and BrOA-2 stations in the lower zone of Patos Lagoon Estuary

Station	Mean	Summer	Autumn	Winter	Spring
BrOA-1 <sub>inner</sub>	9.53	4.18	10.44	10.56	10.79
BrOA-2 <sub>outer</sub>	6.51	0.58	7.72	9.76	5.58

### 3.4. Drivers of pH

The constant effect of TA and DIC on pH was predominant in both stations, with a slightly higher difference in the BrOA-1 station. In both stations, the autumn season presented a uniformity in the pH sensitivity to the variation of its four drivers. The summer season registered the highest sensitivity associated mainly with the increase in DIC with negative effects on the pH, being compensated with the increase in TA. In an antagonistic way, a positive effect due to a decrease in DIC and a negative effect due to a decrease in TA (Fig. 6) was related to the negative seasonal variations of both parameters based on their annual mean (Fig. S.1). This disparity was substantially observed between summer and winter in the BrOA-1 station (Fig. 6A) and summer with both winter and spring in the BrOA-2 (Fig. 6B).

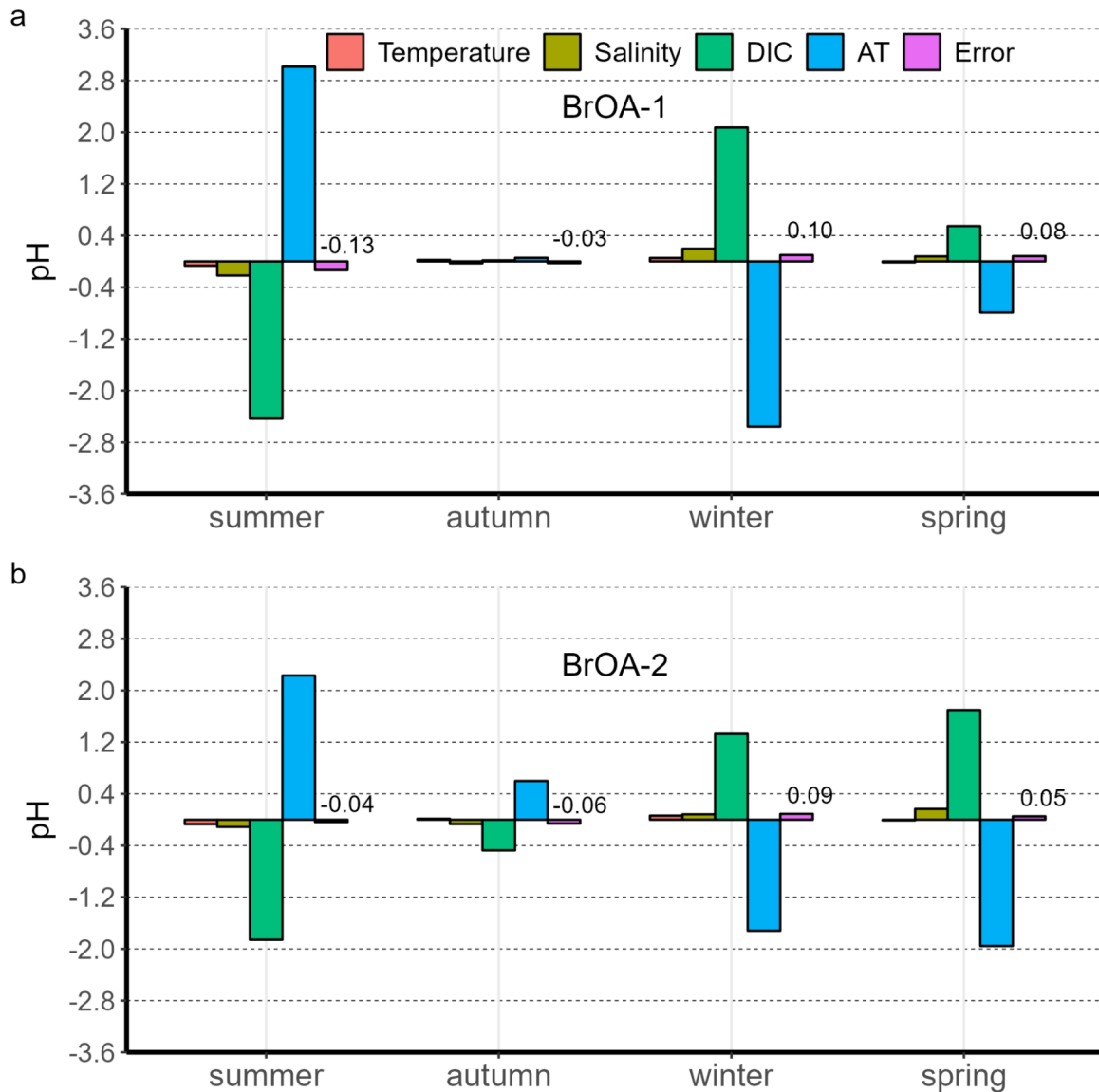


Figure 6. Seasonal effect of temperature, salinity, dissolved inorganic carbon (DIC), and total alkalinity (TA) on surface pH for BrOA-1 (A) and BrOA-2 (B) stations in the lower zone of Patos Lagoon Estuary. The error bar (purple) accompanied by its numerical value shows the difference between the current pH variation and the sum of all the drivers.

#### 4. Discussion

The carbonate system parameters in the lower zone of the PLE were subject to seasonal effects, with significant temporal variability only observed at the inner station (BrOA-1), particularly between summer and both winter and spring. The increased riverine input during the second half of the year did not induce significant seasonal variations in salinity, pH, and TA at the outer station (BrOA-2).

Nevertheless, the corrosive conditions witnessed during winter sharply contrasted with the supersaturation experienced in summer. The pH buffering capacity displayed a consistent pattern throughout the seasons, in contrast to the substantial variability observed between summer and winter in the inner zone. These differences can be attributed primarily to pronounced temporal shifts in salinity resulting from dilution and salinization processes, as indicated by Albuquerque et al. (2022).

The interplay between riverine and oceanic dynamics in the lower estuary suggests an influence on the spatial variations of pH. This difference was most evident between low and high salinities at the outer station, standing in contrast to the inner station, where pH at low salinity significantly deviated from the overall gradient. The TA,  $\Omega_{Ar}$ ,  $\beta$ DIC showed dissimilarity in low, medium, and high salinities within each station, presenting spatial discrepancy in the buffer capacity at lower salinity. Within this range,  $p\text{CO}_2$ , pH, and  $\text{CO}_3^{2-}$  exhibited heightened sensitivity to DIC additions compared to the two estuarine systems with high and moderate buffer capacity river inputs simulated by Cai et al. (2021). This amplified sensitivity, particularly in low salinity may suggest a moderate to low resilience of pH for a lower zone of PLE.

The inner station's higher (lower) buffering capacity (sensitivity) at low salinity can be linked to its elevated value of the Maximum Estuarine Acidification salinity, reflecting a broader salinity range encompassing values below this equilibrium point. Within this range, DIC dissolves into the existing aqueous  $\text{CO}_2$  pool, which increases as it diverges from the MEA salinity. Consequently, the impact of DIC additions on pH diminishes (Hu and Cai, 2013). The seasonal differences of MEA salinity in each station were associated with the results of the effects of each environment driver on pH, particularly in the summer where the predominant TA positive and DIC negative effect by seawater input, supported the lower MEA salinity for both regions.

The marked seasonal influence of the endmembers, mainly in summer and winter was more evident in the monthly variability of the  $\beta$ DIC and salinity, with high and constant records of buffering capacity above its mean ( $105 \mu\text{mol kg}^{-1}$ ) in the first semester in the outer station in opposition to continuous drop from February to August in the inner stations. The period of August to November of low salinity (mean < 10) recorded the lowest buffer capacity in both stations with little similarity with the salinity, being more comparable with the variability of chlorophyll. These results are supported by the conceptual models of Duarte et al. (2013) and Carstensen & Duarte (2019), which define the influence of endmembers and ecosystem metabolism as regulatory components in coastal ecosystems.

A comparative starting point for estimating the buffering level of the lower zone of PLE was the evaluation of  $\beta$ DIC of its endmember. The ocean buffer capacity of the PLE ( $212 \mu\text{mol kg}^{-1}$ ) fell within the global range estimated for the oceans ( $160\text{--}280 \mu\text{mol kg}^{-1}$ ) according to Takahashi et al. (2014). Contrasting this global estimate, the annual mean values in the lower estuary of Patos Lagoons represented by  $\text{BrOA-1}_{\text{inner}}$  ( $95 \pm 7 \mu\text{mol kg}^{-1}$ ) and  $\text{BrOA}_{\text{outer}}$  ( $106 \pm 11 \mu\text{mol kg}^{-1}$ ) lay below the lower limit observed in oceans (Table 4). On the other hand, the  $\beta$ DIC of the riverine buffer capacity ( $38 \mu\text{mol kg}^{-1}$ ) exhibited similarities with the records derived from the rivers in the Strait of Georgia ( $48$  to  $56 \mu\text{mol kg}^{-1}$ ) as determined by Simpson et al. (2022). The highest seasonal means, both for the inner ( $142 \pm 14 \mu\text{mol kg}^{-1}$ ) and outer ( $134 \pm 22 \mu\text{mol kg}^{-1}$ ) stations, were recorded in summer, however, these values remained below the broader range of  $189\text{--}428 \mu\text{mol kg}^{-1}$  calculated at the same season in the well-buffered lagoonal estuary of Corpus Christi Bay, situated in a semiarid subtropical region (Hu et al., 2017). The stretch between the southwestern passage of the Mississippi to the Texas platform displayed a buffering effect ranging from 160

$\mu\text{mol kg}^{-1}$  (Mississippi River plume) to  $360 \mu\text{mol kg}^{-1}$  in summer, featuring a surface record exceeding  $250 \mu\text{mol kg}^{-1}$  (McCutcheon, 2019). An intriguing scenario unfolded in the estuaries of the northwestern Gulf of Mexico, which exhibited a notably high resilience ( $\sim 201 \mu\text{mol kg}^{-1}$ ) accompanied by a declining trend. Despite this resilience, these estuaries experienced temporal subsaturation conditions with the potential to negatively impact calcifying organisms (McCutcheon and Hu, 2022).

The records of aragonite saturation showed a distribution of corrosive conditions up to medium salinities in the outer zone, different from its counterpart, whose values were observed even in seawater. Other systems, such as the Corpus Christi Bay estuary, did not present aragonite subsaturation conditions throughout its salinity gradient (18.6-39.6) and even at the bottom despite the occurrence of hypoxia (Table 2). This resilience is attributed to the high presence of seagrass meadows and to the strong density resulting from the high evaporation that concludes with the contribution of waters with low  $\text{CO}_2$  in the bottom (McCutcheon, 2019). On the other hand, the buffer capacity in the long coastal plain estuary Delaware was associated with the contribution of high carbonate freshwater attributed to the weathering of limestone and dolomite bedrock, leading to high alkalinity values of the estuary ranging between  $915$  and  $2225 \mu\text{mol kg}^{-1}$  and a pH between 7.1 (salinity  $<2.5$ ) to 8.5 (salinity=25). In addition, the TA and pH of the riverine endmember in the present study ( $588.52 \mu\text{mol kg}^{-1}$  and 7.55) were similar to the pre-established values by Carstensen & Duarte (2019) to simulate a coastal ecosystem influenced by freshwater endmember with a lower buffer capacity (TA= $400 \mu\text{mol kg}^{-1}$  and pH=7), and less than the calculated alkalinity for the three endmembers of the Delaware estuary, with approximate means of  $881 \mu\text{mol kg}^{-1}$ ,  $1572 \mu\text{mol kg}^{-1}$  and  $1093 \mu\text{mol kg}^{-1}$ .

kg<sup>-1</sup> for the Trenton, Schuylkill and Christina rivers, respectively (Cyronak et al., 2018).

Table 2. Buffer capacity of pH to fractional change of dissolved inorganic carbon ( $\beta$ DIC) in coastal ecosystems and ocean. The table displays the mean or range report of salinity, total alkalinity (TA), pH at total scale, state of aragonite saturation ( $\Omega$ Ar), partial pressure of carbon dioxide ( $p$ CO<sub>2</sub>), dissolved inorganic carbon (DIC), and  $\beta$ DIC. BrOA-1 and BrOA-2 represent, respectively, the conditions at the inner and outer zones of the Patos Lagoon Estuary (PLE).

System	Salinity (unitless)	TA ( $\mu$ mol kg <sup>-1</sup> )	pH (total scale)	$\Omega$ Ar (unitless)	$p$ CO <sub>2</sub> ( $\mu$ atm)	DIC ( $\mu$ mol kg <sup>-1</sup> )	$\beta$ DIC ( $\mu$ mol kg <sup>-1</sup> )
<i>PLE (2017-2022) [this research]</i>							
<b>BrOA-1</b>	16	1230	7.73	0.9	656	1167	95
Summer	23	1653	7.89	1.64	517	1514	142
<b>BrOA-2</b>	15	1270	7.83	1.17	520	1176	105
Summer	19	1556	7.99	1.65	432	1417	134
<i>Ocean [Takahashi et al., 2014]</i>							
Global mean	35.1	2308	8.09	3.7	347	1978	160-280
<i>Corpus Christi bay (summer) [McCutcheon et al., 2019]</i>							
2015	27.7	2561	8.11	4.93	384.7	2159	284
2016	32.3	2409	8.09	4.47	378.3	2023	287
<i>Mississippi-Texas (24-31/06/2010) [Hu et al., 2017]</i>							
N/A	16-37	2450	8.04-8.47	3.9-8.1	—	—	160-360
<i>Estuaries in the northwestern Gulf of Mexico [McCutcheon and Hu, 2022]</i>							
Sabine-Neches	6.7	973	7.28	0.2	2377	1043	100
Trinity-San Jacinto	20.2	2050	7.98	2.7	580	1899	160
Lavaca-Colorado	25	2335	8.01	2.5	577	2131	200
Guadalupe	22	2563	8.05	3.8	641	2428	220
Mission-Aransas	24.9	2523	8.04	3.2	584	2291	220
Nueces	31.2	2537	7.99	3.2	608	2279	240
Laguna Madre	33.7	2792	8.05	4.2	626	2437	290
<i>Strait of Georgia (2015-2018) [Simpson et al., 2022]</i>							
Theodisia <sub>river</sub>	6.75	589	7.39	0.04	691	625	48
Tokenatch <sub>river</sub>	0.06	116	6.81	0	859	169	56
Puntledge <sub>river</sub>	1.84	387	7.21	0.01	889	436	53
Malaspina <sub>inlet</sub>	25.71	1798	8.11	1.91	284	1630	160
N-SOG	27.5	1948	7.99	1.45	412	1826	141

A straightforward projection of pH response based on DIC alterations was derived from its sensitivity factor ( $SF = \partial pH / \partial DIC$ ), yielding an annual average variation of  $-0.007$  pH units over the 2017-2022 timeframe (see Table S.4). This value fell below the projected trend for coastal ecosystems ( $-0.023$  to  $0.023$  pH units yr<sup>-1</sup>) as

estimated by Carstensen & Duarte (2019). Furthermore, it was consistent with the prevailing trend of  $-0.0002$  to  $-0.0225$  pH units  $\text{yr}^{-1}$  observed in the shallow lagoonal estuaries of the northwestern Gulf of Mexico. These estuaries experienced continuous pH fluctuations attributed to an imbalance in their net ecosystemic metabolism due to the dual influences of warming and ocean acidification (McCutcheon and Hu, 2022).

The seasonal disparity of the influence of each environmental driver on the pH could be attributed to the influx of freshwater and seawater, with the inner zone being more susceptible to seasonal pH change. The summer registered the highest sensitivity associated mainly with the increase of the negative effect of DIC on the pH, being compensated by the positive effect of the TA. The antagonistic effect was observed during the winter, when freshwater discharge is slightly higher leading to a decrease in DIC and TA in the inner zone (Albuquerque et al., 2022). Similarly, the outer zone showed susceptibility to changes in pH during the spring, which had the highest negative anomalies of salinity, DIC, and TA (Fig.S.1). This could be explained by the increase in the intensity of the northeastern winds at the end of winter and spring, which contributes to a greater entrance of freshwater to this zone, strengthening the dilution process that together with the concentration of salts were identified as the main drivers of the variability of carbonate system parameters in the surface water of the lower estuarine zone (Albuquerque et al., 2022).

## **5. Concluding remarks**

The present study is one of the few and first investigations focused on determining, evaluating, and quantifying the sensitivity (tendency to change) and buffering capacity (resistance to change) mainly of pH to the alteration of DIC. The

methodology involved the concept of maximum estuarine acidification salinity as a breaking point where the pH is more susceptible to additions of CO<sub>2</sub> of natural or anthropogenic origin. This study also considered the seasonal variability of the carbonate system parameters and the effect of each environmental driver on the seasonal variability pH, which was quantified and expressed in pH units. The processes of dissolution and concentrations of salts marked the seasonal variations, particularly during the summer, where the seasonal predominant TA positive and DIC negative effect by seawater input, supported the lower MEA salinity for both stations monitoring.

The lower zone of the PLE was characterized by a wide range of alkalinity and alkaline pH conditions, with riverine input with low buffering, and susceptible to corrosive conditions in medium and high salinities. Based on the conceptual models that explain the variability of pH in coastal ecosystems, the salinity (as a proxy of endmembers) and Chl-a (as a proxy for biological activity) were analyzed with the dynamics of the buffer factor clearly showing an increase or decrease with the variability of the salinity. Nevertheless, during the months when salts are most diluted by continental input, photosynthetic activity becomes more prominent.

Since there is limited research that quantifies buffer capacity and no established limit that defines buffering levels, the buffer capacity of the estuary stations could only be inferred by comparison to other systems, suggesting a moderate-low buffer capacity. The relevance of Patoos Lagoon estuary as the largest hatchery of pink shrimp post-larvae in the southern and southeastern regions of Brazil (D'Incao, 1991), supports the demand for a comprehensive knowledge of its biogeochemical estuarine, which will help to determine temporal and spatial trends and develop

strategies and climate prevention or mitigation plans to an ecosystem with low/moderate buffering ability that is also vulnerable to anthropogenic pressure.

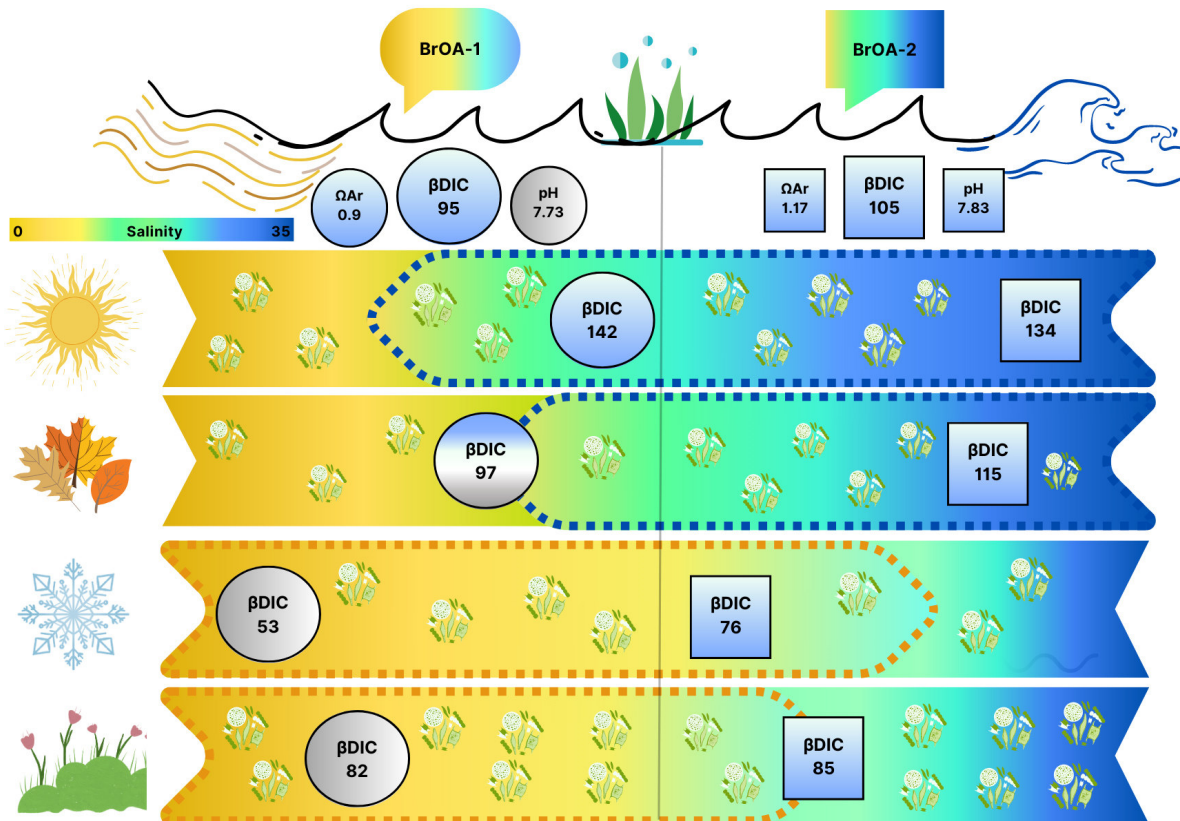


Figure 7. Schematic representation of the seasonal variability of the buffering capacity in the lower zone of Patos Lagoon Estuary. The means of the state of aragonite saturation ( $\Omega_{Ar}$ ), buffering capacity of pH ( $\beta DIC$ ), and pH are displayed upper of the seasonal means of  $\beta DIC$  at summer (sun), autumn (leaves), winter (ice crystal), and spring (flowers). The colors utilized (blue and grey) emphasize spatial discrepancies in pH and seasonal variations in  $\beta DIC$  at the inner station BrOA-1. The salinity gradient color and dotted arrows represent the seasonal influence of the freshwater (brown to yellow) and seawater (blue to green) endmembers in the inner (BrOA-1) and outer (BrOA-2) environments of the studied region.

### Declaration of competing interest

The authors declare that they have no known competing financial interests or personal relationships that could have appeared to influence the work reported in this paper.

## **Data availability**

Data will be made available on request.

## **Acknowledgments**

The database used was generated from the monitoring programs of the Brazilian Ocean Acidification Network (BrOA; [www.broa.furg.br](http://www.broa.furg.br)) and the Patos Lagoon Brazilian Long-Term Ecological Research Program (database available at <https://doi.org/10.15468/xmlvxm>). The study received financial support from the CARBON-FLUX (National Council for Scientific and Technological Development – CNPq grant no. 420118/2018–7) and MICROBIO-ELP (CNPq grant no. 404415/2021-0) projects. P. Quintana and A. Piñango received MSc (no. 88887.597967/2021-00) and PhD (no. 88887.655449/2021-00) grants from the Coordenação de Aperfeiçoamento de Pessoal de Nível Superior (CAPES), respectively. R. Kerr received a CNPq researcher grant no. 309978/2021-1. We also acknowledge the resources provided by CAPES to support the Graduate Program in Oceanology and free access to many scientific journals through *Periódicos* CAPES. Joe Macalupú Rosado from the Institute of Sea of Peru and Carlos Rafael B. Mendes from FURG are acknowledged for their support in preparing the map of the study area and dissolved nutrients analysis, respectively. Finally, we thank all the students, technicians, and researchers involved in the different monitoring programs in the Patos Lagoon Estuary.

## 6. Supplementary material

Table S.1. Mean and standard error of the propagated uncertainties in the calculation of the carbon dioxide system in the lower estuary for each season. The unit of each uncertainty corresponds to the unit of each evaluated variable: DIC ( $\mu\text{mol kg}^{-1}$ ),  $p\text{CO}_2$  ( $\mu\text{atm}$ ),  $\Omega\text{Ar}$  (unitless),  $\text{CO}_2$  ( $\mu\text{mol kg}^{-1}$ ),  $\text{CO}_3^{2-}$  ( $\mu\text{mol kg}^{-1}$ ).

Variable	Mean	Summer	Autumn	Winter	Spring
DIC	$13.99 \pm 0.67$	$18.50 \pm 1.31$	$14.26 \pm 1.26$	$9.32 \pm 0.94$	$12.99 \pm 1.36$
$p\text{CO}_2$	$75.07 \pm 3.02$	$63.94 \pm 3.95$	$69.34 \pm 4.95$	$78.46 \pm 5.01$	$96.94 \pm 10.28$
$\Omega$ Aragonite	$0.10 \pm 0.007$	$0.17 \pm 0.01$	$0.11 \pm 0.01$	$0.04 \pm 0.01$	$0.09 \pm 0.01$
$\Omega$ Calcite	$0.17 \pm 0.012$	$0.27 \pm 0.02$	$0.17 \pm 0.02$	$0.07 \pm 0.01$	$0.14 \pm 0.02$
$\text{CO}_2$	$2.86 \pm 0.12$	$1.95 \pm 0.11$	$2.75 \pm 0.21$	$3.45 \pm 0.21$	$3.63 \pm 0.41$
$\text{CO}_3^{2-}$	$6.69 \pm 0.50$	$10.56 \pm 0.90$	$6.87 \pm 0.92$	$3.03 \pm 0.71$	$5.51 \pm 1.05$

Table S.2. Means ( $\pm$  standard error) and two-way ANOVA results for six parameters of the carbonate system (salinity, TA, pH,  $\Omega$ Ar,  $p\text{CO}_2$ ,  $\beta\text{DIC}$ ) recorded seasonally at two monitoring stations (BrOA-1<sub>inner</sub> and BrOA-2<sub>outer</sub>) in the lower estuary of Patos Lagoon. Results of two-way ANOVA are displayed in the third set of lines. Asterisks indicate significance of ANOVA (\* =  $p < 0.05$ , \*\* =  $p < 0.01$ , \*\*\* =  $p < 0.001$ , ns: non-significant). Different letters indicate significant differences ( $p < 0.05$ ) between the seasons within stations, evaluated with post-ANOVA Tukey's tests at a significance level of  $p < 0.05$ . Lowercase letters denote seasonal means and capital letters represent station means.

Station Season	<i>n</i>	Salinity	pH (total scale)	TA ( $\mu\text{mol kg}^{-1}$ )	$\Omega$ Ar	$p\text{CO}_2$ ( $\mu\text{atm}$ )	$\beta\text{DIC}$ ( $\mu\text{mol kg}^{-1}$ )
BrOA-1	112	15 $\pm$ 1 <sup>A</sup>	7.73 $\pm$ 0.02 <sup>A</sup>	1230 $\pm$ 54 <sup>A</sup>	0.90 $\pm$ 0.10 <sup>A</sup>	656 $\pm$ 34 <sup>A</sup>	95 $\pm$ 6 <sup>A</sup>
Summer	28	23 $\pm$ 2 <sup>a</sup>	7.89 $\pm$ 0.03 <sup>a</sup>	1653 $\pm$ 109 <sup>a</sup>	1.64 $\pm$ 0.20 <sup>a</sup>	517 $\pm$ 39 <sup>a</sup>	142 $\pm$ 14 <sup>a</sup>
Autumn	33	16 $\pm$ 1 <sup>ab</sup>	7.78 $\pm$ 0.05 <sup>ab</sup>	1237 $\pm$ 95 <sup>ab</sup>	0.97 $\pm$ 0.21 <sup>ab</sup>	579 $\pm$ 56 <sup>ab</sup>	97 $\pm$ 12 <sup>ab</sup>
Winter	26	8 $\pm$ 1 <sup>b</sup>	7.60 $\pm$ 0.04 <sup>b</sup>	870 $\pm$ 62 <sup>b</sup>	0.27 $\pm$ 0.09 <sup>b</sup>	692 $\pm$ 57 <sup>ab</sup>	53 $\pm$ 6 <sup>b</sup>
Spring	25	12 $\pm$ 2 <sup>b</sup>	7.64 $\pm$ 0.06 <sup>b</sup>	1118 $\pm$ 112 <sup>b</sup>	0.62 $\pm$ 0.17 <sup>b</sup>	874 $\pm$ 102 <sup>b</sup>	82 $\pm$ 11 <sup>ab</sup>
BrOA-2	66	16 $\pm$ 1 <sup>A</sup>	7.83 $\pm$ 0.04 <sup>B</sup>	1270 $\pm$ 83 <sup>A</sup>	1.17 $\pm$ 0.17 <sup>A</sup>	520 $\pm$ 34 <sup>B</sup>	105 $\pm$ 10 <sup>A</sup>
Summer	16	19 $\pm$ 3 <sup>a</sup>	7.99 $\pm$ 0.05 <sup>a</sup>	1556 $\pm$ 166 <sup>a</sup>	1.65 $\pm$ 0.33 <sup>a</sup>	432 $\pm$ 54 <sup>a</sup>	134 $\pm$ 22 <sup>a</sup>
Autumn	23	18 $\pm$ 2 <sup>a</sup>	7.85 $\pm$ 0.07 <sup>a</sup>	1346 $\pm$ 141 <sup>a</sup>	1.30 $\pm$ 0.32 <sup>ab</sup>	500 $\pm$ 54 <sup>a</sup>	115 $\pm$ 19 <sup>a</sup>
Winter	14	13 $\pm$ 3 <sup>a</sup>	7.68 $\pm$ 0.07 <sup>a</sup>	1049 $\pm$ 181 <sup>a</sup>	0.66 $\pm$ 0.28 <sup>b</sup>	525 $\pm$ 41 <sup>a</sup>	76 $\pm$ 19 <sup>a</sup>
Spring	13	10 $\pm$ 3 <sup>a</sup>	7.78 $\pm$ 0.11 <sup>a</sup>	1018 $\pm$ 156 <sup>a</sup>	0.90 $\pm$ 0.89 <sup>ab</sup>	658 $\pm$ 120 <sup>a</sup>	85 $\pm$ 21 <sup>a</sup>
Spatial effect		<b>ns</b>	*	<b>ns</b>	<b>ns</b>	**	<b>ns</b>
Seasonal effect		***	***	***	***	**	***
Interaction		<b>ns</b>	<b>ns</b>	<b>ns</b>	<b>ns</b>	<b>ns</b>	<b>ns</b>

Table S.3. Mean values ( $\pm$  standard error) and results of two-way ANOVA for five parameters of carbonate system (pH, TA,  $\Omega$  Ar,  $p\text{CO}_2$ ,  $\beta\text{DIC}$ ) recorded within different salinity ranges at two monitoring stations (BrOA-1<sub>inner</sub> and BrOA-2<sub>outer</sub>) in the lower zone of Patos Lagoon Estuary. Results of two-way ANOVA are displayed in the third set of lines. Asterisks indicate significance of ANOVA (\* =  $p < 0.05$ , \*\* =  $p < 0.01$ , \*\*\* =  $p < 0.001$ , ns: non-significant). Different lowercase letters indicate significant differences ( $p < 0.05$ ) between salinity ranges within the stations (low: 0-10, medium: 11-25, and high: >25), evaluated with Tukey's post-ANOVA tests at a significance level of  $p < 0.05$ . Lowercase letters denote range salinity means and capital letters represent station means.

Season	n	pH	TA ( $\mu\text{mol kg}^{-1}$ )	$\Omega$ Ar	$p\text{CO}_2$ ( $\mu\text{atm}$ )	$\beta\text{DIC}$ ( $\mu\text{mol kg}^{-1}$ )
BrOA-1	112	7.73 $\pm$ 0.02 <sup>A</sup>	1230 $\pm$ 54 <sup>A</sup>	0.90 $\pm$ 0.10 <sup>A</sup>	656 $\pm$ 34 <sup>A</sup>	95 $\pm$ 6 <sup>A</sup>
Low	53	7.58 $\pm$ 0.03 <sup>a</sup>	736 $\pm$ 22 <sup>a</sup>	0.16 $\pm$ 0.02 <sup>a</sup>	773 $\pm$ 56 <sup>a</sup>	43 $\pm$ 2 <sup>a</sup>
Medium	33	7.81 $\pm$ 0.03 <sup>b</sup>	1342 $\pm$ 49 <sup>b</sup>	0.86 $\pm$ 0.08 <sup>b</sup>	537 $\pm$ 39 <sup>a</sup>	58 $\pm$ 2 <sup>b</sup>
High	26	7.96 $\pm$ 0.05 <sup>b</sup>	2094 $\pm$ 35 <sup>c</sup>	2.44 $\pm$ 0.22 <sup>c</sup>	567 $\pm$ 68 <sup>a</sup>	173 $\pm$ 9 <sup>c</sup>
BrOA-2	66	7.83 $\pm$ 0.04 <sup>B</sup>	1270 $\pm$ 83 <sup>A</sup>	1.17 $\pm$ 0.17 <sup>A</sup>	520 $\pm$ 34 <sup>B</sup>	105 $\pm$ 10 <sup>A</sup>
Low	24	7.67 $\pm$ 0.05 <sup>a</sup>	650 $\pm$ 28 <sup>a</sup>	0.17 $\pm$ 0.04 <sup>a</sup>	559 $\pm$ 47 <sup>a</sup>	36 $\pm$ 2 <sup>a</sup>
Medium	11	7.91 $\pm$ 0.10 <sup>ab</sup>	1237 $\pm$ 65 <sup>b</sup>	1.05 $\pm$ 0.23 <sup>b</sup>	497 $\pm$ 123 <sup>a</sup>	93 $\pm$ 9 <sup>b</sup>
High	31	8.01 $\pm$ 0.05 <sup>b</sup>	2084 $\pm$ 30 <sup>c</sup>	2.52 $\pm$ 0.28 <sup>c</sup>	479 $\pm$ 48 <sup>a</sup>	200 $\pm$ 13 <sup>c</sup>
Spatial effect		*	ns	ns	**	ns
Salinity effect		***	***	***	**	***
Interaction		ns	ns	ns	ns	*

Table S.4. Constant effect or sensitivity factor of the temperature, salinity, DIC, and TA on pH.

Parameter	Ocean [Takahashi et., 2014]	Ocean endmember	BrOA-1 (inner)	BrOA-2 (outer)
$\partial\text{pH}/\partial\text{T}$ ( $^{\circ}\text{C}$ ) <sup>-1</sup>	-0.016	-0.014	-0.012	-0.012
$\partial\text{pH}/\partial\text{Sal}$	-0.0125	-0.0124	-0.027	-0.031
$\partial\text{pH}/\partial\text{DIC}$ ( $\mu\text{mol kg}^{-1}$ ) <sup>-1</sup>	-0.0019	-0.0020	-0.0070	-0.0077
$\partial\text{pH}/\partial\text{TA}$ ( $\mu\text{mol kg}^{-1}$ ) <sup>-1</sup>	+0.0018	+0.0020	+0.0071	+0.0077

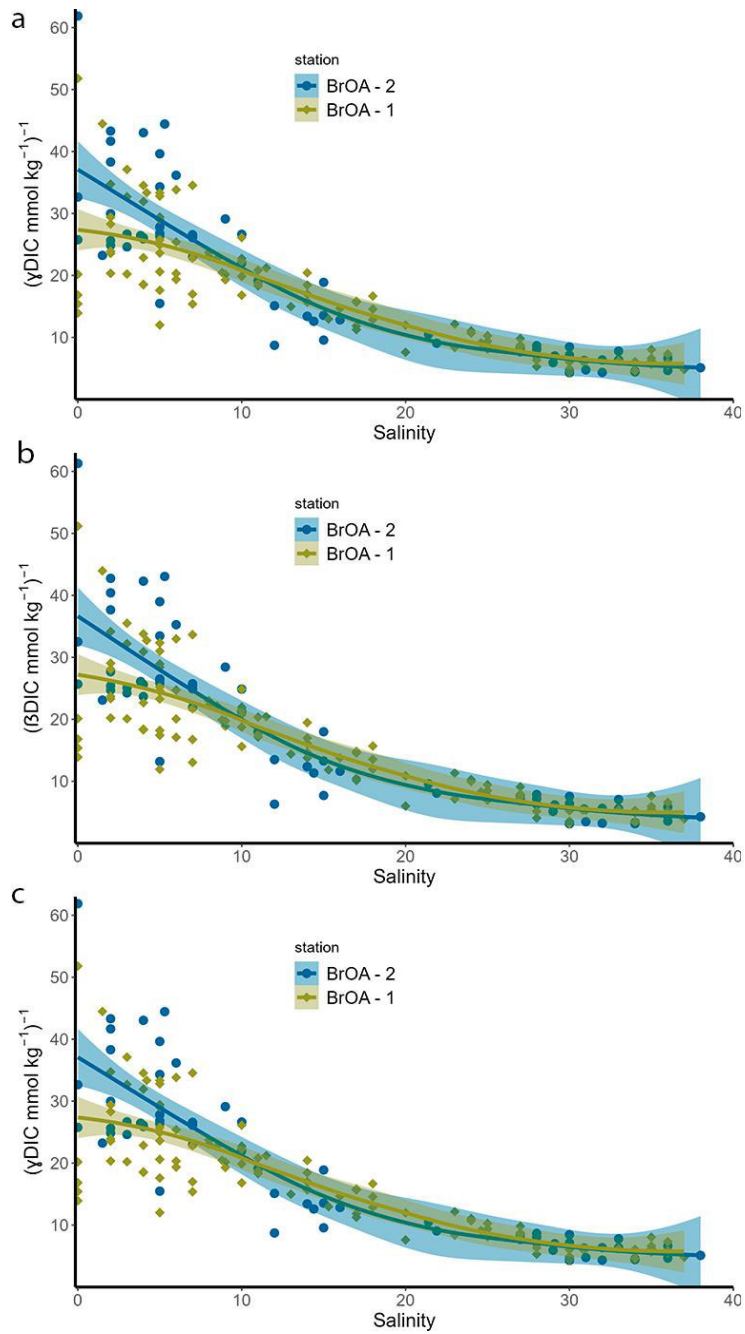


Figure S.1. Rate of change or sensitivity factor of  $p\text{CO}_2$  (a), pH (b), and  $\text{CO}_3^{2-}$  (c) per DIC unit throughout the salinity gradient at the BrOA-1 (yellow) and BrOA-2 (blue) stations in the lower zone of Patos Lagoon Estuary. Each sensitivity factor graphic displays the scattering of its data points along its fit using a weighted least squares regression accompanied by confidence bands for each station.

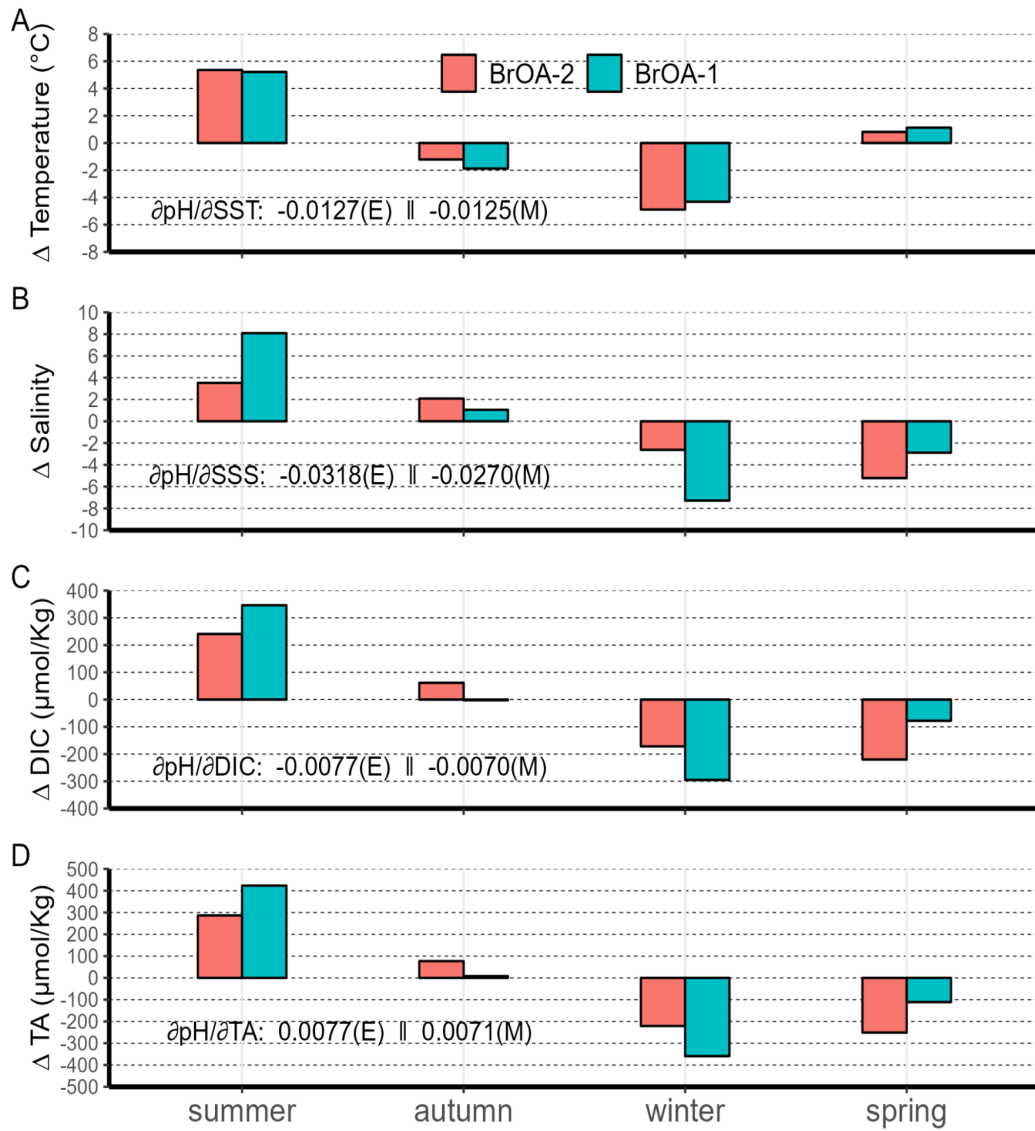


Figure S.2. Seasonal variation of temperature ( $^{\circ}\text{C}$ ), salinity, total alkalinity ( $\mu\text{mol kg}^{-1}$ ), and dissolved inorganic carbon ( $\mu\text{mol kg}^{-1}$ ) relative to their annual means.

# Capítulo VI: Síntese da Discussão e Conclusões

O presente estudo representa uma das primeiras investigações focalizadas na determinação, avaliação e quantificação da sensibilidade (tendência à mudança) e capacidade tampão (resistência à mudança) principalmente do pH, diante da alteração no DIC. A metodologia adotada englobou três conceitos chaves: (i) a salinidade de máxima de acidificação estuarina, que atua como um ponto de ruptura onde o pH é mais suscetível a adição de CO<sub>2</sub> de origem natural ou antropogênico, (ii) a variabilidade sazonal dos parâmetros do sistema de carbonato e (iii) o efeito de cada forçante ambiental ou *driver* na variabilidade sazonal do pH, quantificado e expresso em unidades de pH. Os processos de dissolução e concentração de sais marcaram as variações sazonais, particularmente durante o verão, quando o efeito positivo da TA e o efeito negativo do DIC causado pela entrada de água do mar, sustentando a menor salinidade do MEA para ambas estações de monitoramento.

O baixo estuário foi caracterizado por uma ampla variação nas condições de alcalinidade e um pH alcalino, com aporte ribeirinho apresentando baixo tamponamento e sendo suscetível a condições corrosivas em salinidades médias e altas. Apesar de ambas estações de amostragem estarem situadas

no baixo estuário, sua interação contínua e predominante com diferentes *endmembers* resultou em diferentes resiliências sazonais, especialmente em situações de baixas salinidades, quando a zona interna exibiu maior resiliência. Com base nos modelos conceituais que explicam a variabilidade do pH nos ecossistemas costeiros, a salinidade (como proxy dos *endmembers*) e a Chl-a (como proxy da atividade biológica) foram analisadas em relação à dinâmica do fator tampão, revelando claramente um aumento ou diminuição em resposta à variação da salinidade. No entanto, durante os meses em que os sais são mais diluídos pela entrada continental, a atividade fotossintética torna-se mais proeminente.

Dado o escasso número de pesquisas que quantificam a capacidade de tamponamento e a ausência de limites estabelecidos para definir os níveis de tamponamento, a capacidade tampão das estações estuarinas só pode ser inferida por meio de comparação com outros sistemas, indicando uma capacidade tampão moderada a baixa. A relevância do estuário da Lagoa dos Patos como o maior incubatório de pós-larvas de camarão rosa nas regiões Sul e Sudeste do Brasil (D'Incao, 1991) reforça a necessidade de um entendimento abrangente de sua dinâmica biogeoquímica. Isso não apenas ajudará a determinar as tendências temporais e espaciais, mas também a desenvolver estratégias e planos de prevenção ou mitigação climática para um ecossistema com capacidade tampão baixa a moderada, que também é vulnerável à pressão antropogênica.

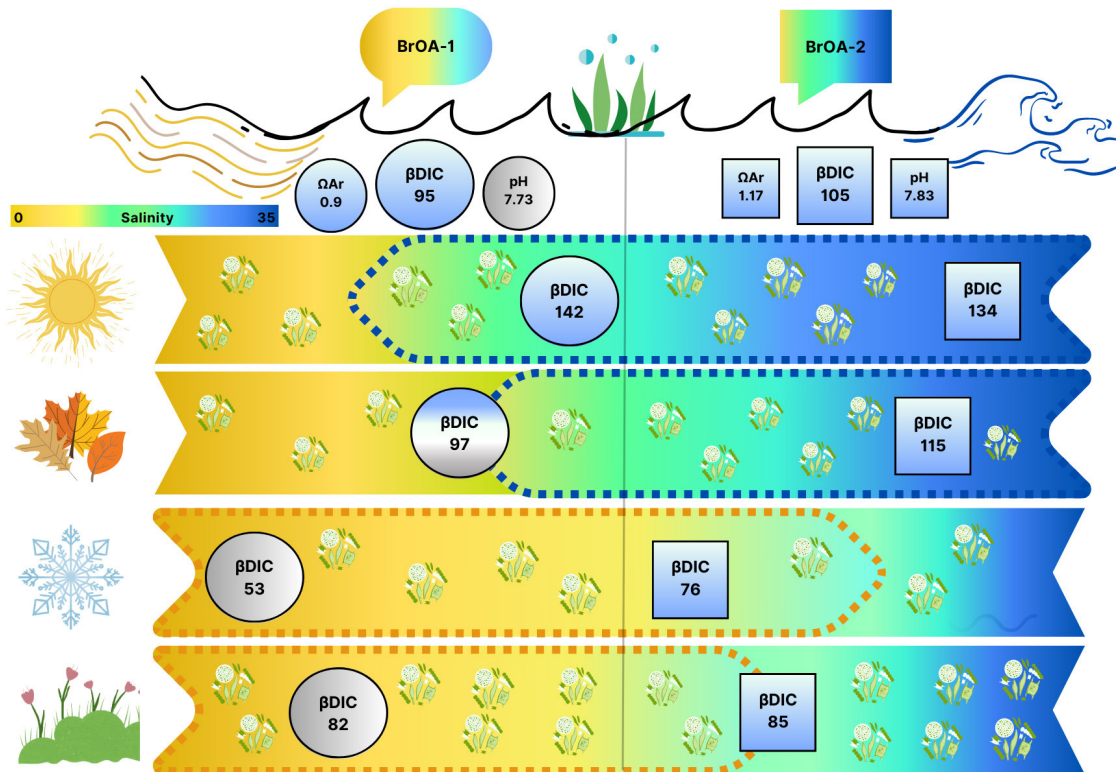


Figura 1. Representação esquemática da variabilidade sazonal da capacidade tampão no baixo estuário da lagoa dos Patos. As médias do estado de saturação da aragonita ( $\Omega_{Ar}$ ), capacidade tampão do pH ( $\beta DIC$ ) e pH são exibidas acima das médias sazonais de  $\beta DIC$  no verão (sol), outono (folhas), inverno (cristal de gelo) e primavera (flores). As cores utilizadas (azul e cinza) enfatizam as discrepâncias espaciais no pH e as variações sazonais no  $\beta DIC$  na estação interna BrOA-1. A cor do gradiente de salinidade e as setas pontilhadas representam a influência sazonal dos membros finais de água doce (marrom a amarelo) e água do mar (azul a verde) nos ambientes interno (BrOA-1) e externo (BrOA-2) da região estudada.

## Referências bibliográficas

Abreu, P. C., Marangoni, J., & Odebrecht, C. (2017). So close, so far: differences in long-term chlorophyll a variability in three nearby estuarine-coastal stations. *Marine Biology Research*, 13(1), 9–21. <https://doi.org/10.1080/17451000.2016.1189081>

Abril, G., Libardoni, B. G., Brandini, N., Cotovicz, L. C., Medeiros, P. R. P., Cavalcante, G. H., & Knoppers, B. A. (2021). Thermodynamic uptake of atmospheric CO<sub>2</sub> in the oligotrophic and semiarid São Francisco estuary (NE Brazil). *Marine Chemistry*, 233. <https://doi.org/10.1016/j.marchem.2021.103983>

Albuquerque, C., Kerr, R., Monteiro, T., de Oliveira Carvalho, A. D. C., da Costa Machado, E., & Mendes, C. R. B. (2023). Seasonal variability in water–air CO<sub>2</sub> exchanges and carbon origin in a subtropical estuary. *Estuarine, Coastal and Shelf Science*, 108457. <https://doi.org/10.1016/j.ecss.2023.108457>

Albuquerque, C., Kerr, R., Monteiro, T., Orselli, I. B. M., Carvalho-Borges, M. de, Carvalho, A. da C. de O., Machado, E. da C., Mansur, J. K., Copertino, M. da S., & Mendes, C. R. B. (2022). Seasonal variability of carbonate chemistry and its controls in a subtropical estuary. *Estuarine, Coastal and Shelf Science*, 276. <https://doi.org/10.1016/j.ecss.2022.108020>

Andrade, M. M., Abreu, P. C., Ávila, R. A., & Möller, O. O. (2022). Importance of winds, freshwater discharge and retention time in the space–time variability of phytoplankton biomass in a shallow microtidal estuary. *Regional Studies in Marine Science*, 50, 102161. <https://doi.org/10.1016/j.rsma.2022.102161>

Baumgarten, M. da G. Z., & Paixão, B. G. da. (2014). Uso do índice do estado trófico para avaliar a qualidade das águas do estuário da lagoa dos Patos (RS). *Atlântica (Rio Grande)*, 35(1), 5–22. <https://doi.org/10.5088/atl.2013.35.1.5>

Bednaršek, N., Newton, J., Beck, M., Alin, S., Feely, R., Christman, N., Klinger, T. (2021). Severe biological effects under present-day estuarine acidification in

the seasonally variable Salish Sea. *Science of the Total Environment*.  
<https://doi.org/10.1016/j.scitotenv.2020.142689>

Bordin, L., Machado, E., Mendes, C., Fernandes, E., Camargo, M., Kerr, R., Schettini, C. (2023). Daily variability of pelagic metabolism in a subtropical lagoonal estuary. *Journal of Marine Systems*, 240.  
<https://doi.org/10.1016/j.jmarsys.2023.103861>.

Cai, W., Feely, R. A., Testa, J. M., Li, M., Evans, W., Alin, S. R., Xu, Y., Pelletier, G., Ahmed, A., Greeley, D. J., Newton, J. A., & Bednaršek, N. (2021). Natural and Anthropogenic Drivers of Acidification in Large Estuaries. 1–33.  
<https://doi.org/10.1146/annurev-marine-010419-011004>

Cai, W., 2011. Estuarine and coastal ocean carbon paradox: CO<sub>2</sub> sinks or sites of terrestrial carbon incineration? *Ann. Rev. Mar. Sci* 3, 123–145  
<https://doi.org/10.1146/annurev-marine-120709-142723>

Carstensen, J., & Duarte, C. M. (2019). Drivers of pH Variability in Coastal Ecosystems [Review-article]. *Environmental Science and Technology*, 53(8), 4020–4029. <https://doi.org/10.1021/acs.est.8b03655>

Cotovicz, L. C., Knoppers, B. A., Régis, C. R., Tremmel, D., Costa-Santos, S., & Abril, G. (2021). Eutrophication overcoming carbonate precipitation in a tropical hypersaline coastal lagoon acting as a CO<sub>2</sub> sink (Araruama lagoon, SE Brazil). *Biogeochemistry*, 156(2), 231–254. <https://doi.org/10.1007/s10533-021-00842-3>

Cotovicz, L. C., Knoppers, B. A., Brandini, N., Poirier, D., Costa Santos, S. J., & Abril, G. (2018). Aragonite saturation state in a tropical coastal embayment dominated by phytoplankton blooms (Guanabara Bay - Brazil). *Marine Pollution Bulletin*, 129(2), 729–739. <https://doi.org/10.1016/j.marpolbul.2017.10.064>

Cyronak, T., Andersson, A. J., D'Angelo, S., Bresnahan, P., Davidson, C., Griffin, A., Kindeberg, T., Pennise, J., Takeshita, Y., & White, M. (2018). Short-Term Spatial and Temporal Carbonate Chemistry Variability in Two

Contrasting Seagrass Meadows: Implications for pH Buffering Capacities. *Estuaries and Coasts*, 41(5), 1282–1296.

<https://doi.org/10.1007/s12237-017-0356-5>

D’Incao, F. (1991). Pesca e biologia de *Penaeus paulensis* na lagoa dos Patos, RS, Brasil. *Atlântica (Rio Grande)* 13(1):159-169.

Dickson, A.G., Sabine, C.L., Christian, J.R., 2007. Guide to Best Practices for Ocean CO<sub>2</sub> Measurements. Sidney, North Pacific Marine Science Organization, p. 191.

Dickson, A. G. (1990). Thermodynamics of the dissociation of boric acid in synthetic seawater from 273.15 to 318.15 K. In *Deep-Sea Research* (Vol. 37, Issue 5).

Duarte, C. M., Hendriks, I. E., Moore, T. S., Olsen, Y. S., Steckbauer, A., Ramajo, L., Carstensen, J., Trotter, J. A., & McCulloch, M. (2013). Is Ocean Acidification an Open-Ocean Syndrome? Understanding Anthropogenic Impacts on Seawater pH. *Estuaries and Coasts*, 36(2), 221–236.

<https://doi.org/10.1007/s12237-013-9594-3>

Egleston, E. S., Sabine, C. L., & Morel, F. M. M. (2010). Revelle revisited: Buffer factors that quantify the response of ocean chemistry to changes in DIC and alkalinity. *Global Biogeochemical Cycles*, 24(1), 1–9.

<https://doi.org/10.1029/2008GB003407>

Feely, R. A., Okazaki, R. R., Cai, W. J., Bednaršek, N., Alin, S. R., Byrne, R. H., & Fassbender, A. (2018). The combined effects of acidification and hypoxia on pH and aragonite saturation in the coastal waters of the California current ecosystem and the northern Gulf of Mexico. *Continental Shelf Research*, 152, 50–60. <https://doi.org/10.1016/j.csr.2017.11.002>

Gattuso, J.-P., Epitalon, J.-M., Lavigne, H., Orr, J., Gentili, B., Hofmann, A., Proye, A., Soetaert, K. and Rae, J., 2016. Seacarb: Seawater Carbonate Chemistry. [http://CRAN.R546\\_project.org/package=seacarb](http://CRAN.R546_project.org/package=seacarb).

Gieskes, J.M., 1969. Effect of temperature on the pH of seawater. *Limnol. Oceanogr.* 14, 679–685. <https://doi.org/10.4319/lo.1969.14.5.0679>.

Gordey, A.A., Osadchiev, A.S. Water Exchange between the Patos lagoon and the Atlantic Ocean Through a Narrow Strait. *Oceanology* 62, 171–181 (2022). <https://doi.org/10.1134/S0001437022020072>.

Grasshoff, K., Kremling, K., Ehrhardt, M., 2009. *Methods of Seawater Analysis: Third, Completely Revised and Extended Edition*. *Methods of Seawater Analysis: Third, Completely Revised and Extended Edition* 1–600. <https://doi.org/10.1002/9783527613984>.

Hu, X., Li, Q., Huang, W. J., Chen, B., Cai, W. J., Rabalais, N. N., & Eugene Turner, R. (2017). Effects of eutrophication and benthic respiration on water column carbonate chemistry in a traditional hypoxic zone in the Northern Gulf of Mexico. *Marine Chemistry*, 194, 33–42. <https://doi.org/10.1016/j.marchem.2017.04.004>

Hu, X., & Cai, W. J. (2013). Estuarine acidification and minimum buffer zone - A conceptual study. *Geophysical Research Letters*, 40(19), 5176–5181. <https://doi.org/10.1002/grl.51000>

IPCC, 2021: *Climate Change 2021: The Physical Science Basis*. Contribution of Working Group I to the Sixth Assessment Report of the Intergovernmental Panel on Climate Change [Masson-Delmotte, V., P. Zhai, A. Pirani, S.L. Connors, C. Péan, S. Berger, N. Caud, Y. Chen, L. Goldfarb, M.I. Gomis, M. Huang, K. Leitzell, E. Lonnoy, J.B.R. Matthews, T.K. Maycock, T. Waterfield, O. Yelekçi, R. Yu, and B. Zhou (eds.)]. Cambridge University Press, Cambridge, United Kingdom and New York, NY, USA, In press, doi:10.1017/9781009157896.

Hellings, L., Dehairs, F., van Damme, S., & Baeyens, W. (2001). Dissolved inorganic carbon in a highly polluted estuary (the Scheldt). *Limnology and Oceanography*, 46(6), 1406–1414. <https://doi.org/10.4319/lo.2001.46.6.1406>

Kerr, R., Da Cunha, L.C., Kikuchi, R.K.P., et al., 2016. The Western South Atlantic Ocean in a high-CO<sub>2</sub> world: current measurement capabilities and perspectives. *Environ. Manag.* 57, 740–752. <https://doi.org/10.1007/s00267-015-0630-x>.

Lee, K., Kim, T. W., Byrne, R. H., Millero, F. J., Feely, R. A., & Liu, Y. M. (2010). The universal ratio of boron to chlorinity for the North Pacific and North Atlantic oceans. *Geochimica et Cosmochimica Acta*, 74(6), 1801–1811. <https://doi.org/10.1016/j.gca.2009.12.027>.

Lemke, N., Calliari, L. J., Fontoura, J. A. S., & Aguiar, D. F. (2017). Wave directional measurement in Patos lagoon, RS, Brazil. *Rbrh*, 22(0). <https://doi.org/10.1590/2318-0331.011716053>

Lemos, V. M., Lanari, M., Copertino, M., Secchi, E. R., de Abreu, P. C. O. V., Muelbert, J. H., Garcia, A. M., Dumont, F. C., Muxagata, E., Vieira, J. P., Colling, A., & Odebrecht, C. (2022). Patos lagoon estuary and adjacent marine coastal biodiversity long-term data. *Earth System Science Data*, 14(3), 1015–1041. <https://doi.org/10.5194/essd-14-1015-2022>

Lewis, E., Wallace, D., Allison, L.J., 1998. Program Developed for CO<sub>2</sub> System Calculations, vol. 38. Carbon Dioxide Information Analysis Center, USA.

Marinho, C., Arigony Neto, J., Nicolodi, J. L., Lemke, N., & Fontoura, J. A. S. (2020). Wave regime characterization in the northern sector of Patos lagoon, Rio Grande do Sul, Brazil. *Ocean and Coastal Research*, 68, 1–18. <https://doi.org/10.1590/s2675-28242020068295>

McCutcheon MR and Hu X. (2022). Long-Term Trends in Estuarine Carbonate Chemistry in the Northwestern Gulf of Mexico. *Frontiers in Marine Science*, 9. <https://doi.org/10.3389/fmars.2022.793065>

McCutcheon, M. R., Staryk, C. J., & Hu, X. (2019). Characteristics of the Carbonate System in a Semiarid Estuary that Experiences Summertime Hypoxia. *Estuaries and Coasts*, 42(6), 1509–1523. <https://doi.org/10.1007/s12237-019-00588-0>

Middelburg, J. J., Soetaert, K., & Hagens, M. (2020). Ocean Alkalinity, Buffering and Biogeochemical Processes. *Reviews of Geophysics*, 58(3). <https://doi.org/10.1029/2019RG000681>

Millero, F. J. (2010). Carbonate constants for estuarine waters. *Marine and Freshwater Research*, 61(2), 139–142. <https://doi.org/10.1071/MF09254>

Möller, O.O., Castaing, P., Salomon, J.C., Lazure, P. (2001). The influence of local and non-local forcing effects on the subtidal circulation of Patos lagoon. *Estuaries* 24, 297–311 (2001). <https://doi.org/10.2307/1352953>

Montero T, Kerr R (2020). Protocolo N° 001. Laboratório de Estudos dos Oceanos e Clima. Instituto de Oceanografia-IO, Universidade Federal do Rio Grande - FURG.

Noriega C, Araujo M (2014) Carbon dioxide emissions from estuaries of northern and northeastern Brazil. *Scientific Reports*, 4. <https://doi.org/10.1038/srep06164>

Odebrecht, C., Abreu, P.C.O.V., 2019. Phytoplankton and water quality parameters in the Patos lagoon estuary and adjacent marine coast. Sistema de Informação sobre a Biodiversidade Brasileira - SiBBr. Sampling event dataset. <https://doi.org/10.15468/xmlvxm> via GBIF.org on 2020-06-09.

Paerl, H. W., Valdes, L. M., Peierls, B. L., Adolf, J. E., & Harding, L. W. (2006). Anthropogenic and climatic influences on the eutrophication of large estuarine

ecosystems. *Limnology and Oceanography*. 2006, 51, 448–462.  
[https://doi.org/10.4319/lo.2006.51.1\\_part\\_2.0448](https://doi.org/10.4319/lo.2006.51.1_part_2.0448)

Pierrot, D., Epitalon, J.-M., Orr, J.C., Lewis, E., and Wallace, D. W. R., MS Excel program developed for CO<sub>2</sub> system calculations – version 3.0, (2021), GitHub repository, [https://github.com/dpierrot/co2sys\\_xl](https://github.com/dpierrot/co2sys_xl)

Seeliger, U. (2001). The Patos lagoon estuary, Brazil. In: Seeliger, U., Kjerfve, B. (eds) *Coastal Marine Ecosystems of Latin America*. Ecological Studies, vol 144. Springer, Berlin, Heidelberg.  
[https://doi.org/10.1007/978-3-662-04482-7\\_13](https://doi.org/10.1007/978-3-662-04482-7_13)

Simpson, E., Ianson, D., & Kohfeld, K. E. (2022). Using End-Member Models to Estimate Seasonal Carbonate Chemistry and Acidification Sensitivity in Temperate Estuaries. In *Geophysical Research Letters* (Vol. 49, Issue 2). John Wiley and Sons Inc. <https://doi.org/10.1029/2021GL095579>

Strickland, J.D.H. and Parsons, T.R. (1972) *A Practical Handbook of Seawater Analysis*. 2nd edition. Ottawa, Canada, Fisheries Research Board of Canada, 310pp. (Bulletin Fisheries Research Board of Canada, Nr. 167 (2nd ed)). DOI: <http://dx.doi.org/10.25607/OBP-1791>

Takahashi, T., Sutherland, S. C., Chipman, D. W., Goddard, J. G., & Ho, C. (2014). Climatological distributions of pH, pCO<sub>2</sub>, total CO<sub>2</sub>, alkalinity, and CaCO<sub>3</sub> saturation in the global surface ocean, and temporal changes at selected locations. *Marine Chemistry*, 164, 95–125.  
<https://doi.org/10.1016/j.marchem.2014.06.004>

Waldbusser, G. G., Bergschneider, H., & Green, M. A. (2010). Size-dependent pH effect on calcification in post-larval hard clam *Mercenaria* spp. *Marine Ecology Progress Series*, 417(x), 171–182. <https://doi.org/10.3354/meps08809>

Welschmeyer, N.A., 1994. Fluorometric analysis of chlorophyll-a in the presence of chlorophyll-b and pheopigments. *Limnol. Oceanogr.* 39, 1985–1992.